UNIVERSITY OF SOUTH BOHEMIA IN ČESKÉ BUDĚJOVICE
INSTITUTE OF PHYSICAL BIOLOGY

Mechanisms involved in sodium uptake activation by the Tumor Necrosis Factor-derived TIP peptide

PhD thesis

Alexander V. Dulebo

Supervisor:
Mgr. David Kaftan, PhD
Institute of Physical Biology, University of South Bohemia in České Budějovice
Nové Hrady, 373 33, Czech Republic

Scientific advisor:
Prof. Rudolf Lucas, PhD
Vascular Biology Center, Georgia Health Sciences University
Augusta, GA 30912-2500, USA

Nové Hrady, 2011

Dulebo, A., 2011: Mechanisms involved in sodium uptake activation by the Tumor Necrosis Factor-derived TIP peptide. PhD thesis, in English – 137 pages, Institute of Physical Biology, University of South Bohemia in České Budějovice, Nové Hrady, Czech Republic.

Prohlašuji, že svoji disertační práci jsem vypracoval samostatně pouze s použitím pramenů a literatury uvedených v seznamu citované literatury.

Prohlašuji, že v souladu s § 47b zákona č. 111/1998 Sb. v platném znění souhlasím se zveřejněním své disertační práce, a to v nezkrácené podobě elektronickou cestou ve veřejně přístupné části databáze STAG provozované Jihočeskou univerzitou v Českých Budějovicích na jejích internetových stránkách, a to se zachováním mého autorského práva k odevzdanému textu této kvalifikační práce. Souhlasím dále s tím, aby toutéž elektronickou cestou byly v souladu s uvedeným ustanovením zákona č. 111/1998 Sb. zveřejněny posudky školitele a oponentů práce i záznam o průběhu a výsledku obhajoby kvalifikační práce. Rovněž souhlasím s porovnáním textu mé kvalifikační práce s databází kvalifikačních prací Theses.cz provozovanou Národním registrem vysokoškolských kvalifikačních prací a systémem na odhalování plagiátů.

V Nových Hradech, dne 7. prosince 2011

Alexander Dulebo

Annotation

The Tumor Necrosis Factor derived-TIP peptide is a small 17 amino acids cyclic peptide with lectin-like activity, that possesses several therapeutically relevant biological activities, among which is activation of alveolar liquid clearance in both healthy and injured lungs *in vivo*. Accumulation of fluid in the lungs' alveoli and interstitial spaces is a life-threatening condition called pulmonary edema. The mortality rate due permeability pulmonary edema, accompanied by a dysfunction of the alveolar/capillary barrier, is high because no effective treatment lacking side effects exists nowadays. It is known that the TIP peptide is able to activate vectorial Na^+ transport – which mediates lung liquid clearance. However, the mechanism of action of remains elusive. The aim of this thesis was to investigate the initial steps of interaction between the TIP peptide and airway epithelial cells. Numerous novel methods and single-molecule techniques were used to unravel: (i) how the TIP peptide interacts with the molecules on the apical side of the lung epithelial cells; (ii) whether the TIP peptide need to be internalized inside of the cells to trigger its effects; (iii) the nature of the interaction between the TIP peptide and its putative receptor(s); (iv) the putative receptor(s) for the TIP peptide on the apical surface of the lung epithelial cells.

Anotace

Cyklický TIP peptid s lektínovou je odvozený ze 17 aminokyselin tumor nekrozního faktoru. Při aktivaci vstřebáváni vody ve zdravých a poškozených plicích *in vivo* hraje významnou medicínsky využitelnou úlohu. Zadržování kapaliny v plicních sklípcích a intersticiálních prostorech je život ohrožující stav zvaný plicní edém. V současné době je vysoká úmrtnost v důsledku plicního edému spojeného s fyziologickou disfunkcí kapilárně alveolární bariéry způsobována především neexistencí účinných léčiv bez vedlejších účinků. Je známo, že TIP peptid je schopen aktivovat transepiteliální transport sodíkových iontů, jenž je primárním procesem vedoucím k odstranění vody z plic. Bohužel, o mechanizmu účinku TIP peptidu není mnoho známo. Cílem této práce bylo zkoumat primární interakci TIP peptidu s plicními epiteliálními buňkami. S použitím široké škály nových metod a přístupů na úrovni jednotlivých molekul jsem zjišťoval (i) jak interaguje TIP peptid s molekulami na apikální straně plicních epiteliálních buněk? (ii) zda je pro aktivaci odstranění plicního edému TIP peptidem nezbytný jeho transport dovnitř epiteliálních buněk? (iii) jaká je povaha interakce TIP peptidu a jeho neznámého receptoru? (iv) jaká molekula slouží jako receptor pro TIP peptid?

List of enclosed publications

I. Hundsberger, H., Verin, A., Wiesner, C., Pflüger, M., **Dulebo, A.**, Schütt, W., Lasters, I., Mannel, N.D., Wendel, A., and Lucas, R. (**2008**) "TNF: a moonlighting protein at the interface between cancer and infection". *Frontiers in Bioscience* **13**, 5374-5386.

II. **Dulebo, A.**, Preiner, J., Kienberger, F., Kada, G., Rankl, C., Chtcheglova, L., Lamprecht, C., Kaftan, D., and Hinterdorfer, P. (**2009**) "Second harmonic atomic force microscopy imaging of live and fixed mammalian cells". *Ultramicroscopy* **109**, 1056-1060.

III. **Dulebo, A.**, Ettrich, R., Lucas, R., and Kaftan, D. (**2011**) "Identification of the oligosaccharide binding sites in the lectin-like domain of tumor necrosis factor: a computational study". *Submitted to Current Pharmaceutical Design.*

IV. **Dulebo, A.**, Lucas, R., and Kaftan, D. "Interaction of the Tumor Necrosis Factor-derived TIP peptide with the surface of H441 lung epithelial cells". *In preparation*.

These publications will be referred in the text by the above Roman numerals.

My contribution to the publications

I have prepared figure in **publication I**. In **publication II** I did the experimental planning, conducted all the experimental work and wrote the entire manuscript. In **publications III** and **IV** I planned all the experiments, performed them alone, and did all the analysis and manuscript writing.

On behalf of the co-authors, the above mentioned declaration was confirmed by:

Mgr. David Kaftan, PhD
(supervisor and co-author of the publications II-IV)

Prof. Rudolf Lucas, PhD
(scientific adviser and co-author of the publications I, III and IV)

Publications not included in the thesis

V. Dinamarca, J., Shlyk-Kerner, O., Kaftan, D., Goldberg, E., **Dulebo, A.**, Gidekel, M., Gutierrez, A., and Scherz, A. (**2011)** "Double mutation in Photosystem II reaction centers and elevated CO_2 grant thermotolerance to mesophilic cyanobacterium". *PLoS ONE in press.*

VI. Kopecký, V., Kohoutová, J., Lapkouski, M., Hofbauerová, K., Sovová, Ž., Ettrichová, O., González-Pérezc, S., **Dulebo, A.**, Kaftan, D., Smatanová, I., Revuelta, J., Arellano, J., and Ettrich, R. "Can drop coating deposition Raman spectroscopy distinguish shortcomings or inaccuracies in protein crystals? Case study of PsbP protein of photosystem II from *Spinacia oleracea*". *Submitted to PLoS ONE.*

VII. Šlouf, V., Fuciman, M., **Dulebo, A.**, Kaftan, D., Koblížek, M., Frank, H.A., and Polívka, T. "Caratenoid-mediated energy transfer in LH1-RC complexes of aerobic anoxygenic phototrophic bacteria". *In preparation*.

VIII. Medová, H., **Dulebo, A.**, Kaftan, D., Boldareva, E., and Koblížek, M. "Excess thermal capacity of bacterial reaction centers". *In preparation*.

IX. Shlyk-Kerner, O., Matěnová, M., Dinamarca, J., **Dulebo, A.**, Scherz, A., and Kaftan, D. "Glycines at the interface of transmembrane helices of D1 and D2 proteins of PSII: structural and functional flexibility versus stability". *In preparation*.

My contribution to the publications

In **publication V** I did molecular dynamics simulation, did the analysis of the simulated structures, and did figures preparation. In **publication VI** I did force spectroscopy measurements, analyzed the data and calculated the dissociation constant. Photosystems comprising of reaction center and its light harvesting complex (LH1-RC) that I have isolated and purified were studied in **publication VII** and **publication VIII**. For **publication IX** I did molecular dynamics simulation and conducted force spectroscopy experiments.

On behalf of the co-authors, the above mentioned declaration was confirmed by:

Mgr. David Kaftan, PhD
(supervisor and co-author of the publications V-IX)

Acknowledgements

This work has been stimulated by novel ideas introduced to me back in the year 2005 by my scientific advisor Prof. Rudolf Lucas, PhD. My fascination for this project has been upheld since then. Apart from sharing with me his sheer knowledge and demonstration new methods, he also taught me the lessons of scientific communication.

I have obtained enormous support and guidance from my supervisor and mentor Mgr. David Kaftan, PhD. Thanks to him I have mastered the skills to conduct research independently. His life experiences that he shared with me make my stay in Czech Republic enriched.

In the process of learning I have been acquiring information, skills and knowledge of techniques which were intensively delivered by means of lectures, seminars, conferences and private communications provided by the academic staff of the Institute of Physical Biology. I have met many interesting people there: outstanding scientists, interesting speakers, good friends of all ages and nationalities. Needless to say that all of them have played an important role in my life and scientific career during the years spent at the Institute of Physical Biology. Especially, I would like to acknowledge the help and guidance of Doc. RNDr. Rüdiger Ettrich, PhD, who has been open for discussions every time I needed it.

The scientific collaborations of my supervisors as well as their generous support allowed me to gain even more knowledge and practical skills by joining various scientific groups abroad. My visits of Univ. Prof. Dr. Peter Hinterdorfer at the Johannes Kepler University in Linz and Prof. Mag. Dr. Harald Hundsberger at the University of Applied Sciences in Krems were very helpful. These visits resulted in join publications which are presented in this thesis. I am very grateful for the help of Dipl. Biol. Maren Pflüger who performed Ussing chamber measurements presented in this thesis.

Although the scientific work was prevailing for the most of the time, the life would be meaningless without close and dearest people who were with me all that time. I am enormously thankful for their support, understanding and belief in me.

Finally, I would like to say that I want to dedicate this thesis to my dear parents Lilia and Victor Dulebo, who educated me, and to Katsiaryna Shimanovitch who introduced the world of science to me.

List of abbreviations

3D	Three-dimensional
AFM	Atomic force microscope (or microscopy)
ALI	Acute lung injury
ARDS	Acute respiratory distress syndrome
cAMP	Cyclic adenosine monophosphate
CD	Cluster of differentiation
ENaC	Epithelial sodium channel
FF	Force field
GTP	Guanosine triphosphate
HEPES	4-(2-hydroxyethyl)-1-piperazineethanesulfonic acid
HH	Higher harmonics
HOPG	Highly ordered (or oriented) pyrolytic graphite
IgM	Immunoglobulin M
kDa	kiloDalton
LLC	Lung liquid clearance
LLO	Listeriolysin
LT-α	lymphotoxin-α
MD	Molecular dynamics
mutTIP	mutated Tumor Necrosis Factor-derived TIP peptide
MVEC	Microvascular endothelial cells
nm	Nanometer
NMR	Nuclear magnetic resonance
OPLS-AA	Optimized potentials for liquid simulations-all atom
PDB	Protein data bank
PEG	Polyethylene glycol
PKC	Protein kinase C
PME	Particle mesh Ewald
pN	piconewton
PTFE	Polytetrafluoroethylene
PVC	Polyvinyl chloride
ROS	Reactive oxygen species
scrTIP	scramble Tumor Necrosis Factor-derived TIP peptide
SDS-PAGE	Sodium dodecyl sulfate polyacrylamide gel electrophoresis
SF	Scoring function
SMFS	Single-molecule force spectroscopy
SNOM	Scanning near-field optical microscopy
SPM	Scanning probe microscopy
STM	Scanning tunneling microscope (or microscopy)
TIP peptide	Tumor Necrosis Factor-derived TIP peptide
TNF	Tumor Necrosis Factor
TNF-R	Tumor Necrosis Factor receptor

Contents

CHAPTER 1 – PREFACE 11

1.1 MOTIVATION 12

1.2 INTRODUCTION 12

1.3 AIMS OF THE THESIS 19

CHAPTER 2 – MATERIALS AND METHODS 29

2.1 SCANNING PROBE MICROSCOPY 30

2.2 SINGLE-MOLECULE FORCE SPECTROSCOPY 38

2.3 MOLECULAR DOCKING 45

2.4 MOLECULAR DYNAMICS SIMULATIONS 52

CHAPTER 3 – RESULTS AND DISCUSSION 59

CHAPTER 4 – CONCLUSION 67

4.1 CONCLUSION 68

4.2 FUTURE WORK 68

CHAPTER 5 – REFERENCES 71

CHAPTER 6 – PAPERS 87

Chapter 1

Preface

1.1 Motivation

"When you cannot breathe, the rest doesn't matter"
-unknown author

The World Health Organization recognizes more than a hundred diseases mankind is suffering from, each of which with a different etiology, scope and complicacy. The possibility to develop a specific therapy to one of them, i.e. pulmonary edema is a major goal of any research. The subject of this thesis represents a part of an ongoing research that aims at resolving the mystery of Na^+ uptake activation mechanism mediated by the Tumor Necrosis Factor (TNF) derived TIP peptide. This uptake of Na^+ is an initial step in a sequence of events leading to improved transepithelial liquid transport, as such clearing pulmonary edema. The mortality of this condition is still high, also due to the lack of side-effect free medication. The TIP peptide, which currently undergoes clinical trials, has shown promising results in resolution of pulmonary edema, making its further study highly important.

1.2 Introduction

1.2.1 TNF: a pleiotropic cytokine

TNF, also known as cachectin, is a pleiotropic cytokine originally known for its role in immune modulation, anti-tumor activity, inflammation, cachexia, septic shock, and hematopoesis activities (Carswell *et al.,* 1975). It is expressed by a large variety of cells, but primarily by activated macrophages, mast cells and T lymphocytes. Since its discovery in 1975, a lot of information has been obtained about TNF's structure (Jones *et al.,* 1989; Eck and Sprang, 1989) and function (Vassalli 1992). TNF is generated as a membrane-bound precursor that is cleaved by the TNF-α converting enzyme, giving rise to the soluble 17 kDa monomer, which needs to form homotrimers in the circulation, in order to become bioactive. The TNF ligand acts by binding to two different TNF receptors (CD120): TNF-R1 (55 kDa), which contains a death domain, which signals for apoptosis and TNF-R2 (75 kDa), containing no death domain (Wallach *et al.,* 1999). At least one of these receptor types is expressed in most somatic cells (Vassalli 1992; Hehlgans and Pfeffer 2005), and kills TNF-sensitive cells by means of apoptosis (Fiers *et al.,* 1995; **publication I**). Mouse and human TNF-α share 79% amino acid sequence identity; however, unlike human TNF-α, the mouse form is glycosylated.

It is generally assumed that biomolecules are very specific both in terms of receptors they bind to and the effects they mediate. However, numerous multifunctional proteins in which two or more different functions are performed by one polypeptide chain were discovered recently (Jeffery 1999). These so-called "moonlighting" proteins seem to be the products of molecular evolution (Piatigorsky 2007). Moonlighting proteins do not include proteins that have multiple functions due to either gene fusions or multiple splice variants. Also, they do not include proteins with the same function in multiple locations, or the protein families where different members have different functions, if each individual has only one function. There are several dozen of proteins in prokaryotes, fungae, plants, and animals that have been found to moonlight. Many proteins that moonlight are enzymes, receptors, ion channels and chaperones (Piatigorsky *et al.,* 1988; Jeffery 1999; Huberts and van der Klei 2010). TNF represents one of the examples of a moonlighting protein (**publication I**).

1.2.2 The lectin-like domain of TNF

Besides its apoptotic and inflammatory activities, TNF was also shown to exert a lytic activity on purified blood forms of African trypanosomes (Lucas *et al.,* 1993; Lucas *et al.,* 1994; Daulouede *et al.,* 2001), an effect that cannot be blocked by soluble TNF-R1, which blocks all the TNF receptor-mediated effects (Lucas *et al.,* 1994). However, specific oligosaccharides, such as *N,N'*-diacetylchitobiose and branched trimannoses, as well as lectins with a similar oligosaccharide specificity as TNF, can block the trypanolytic effect of TNF (Lucas *et al.,* 1994). Another study demonstrated that TNF, upon binding of its lectin-like domain to glycoproteins, still retains its cytotoxic activity in tumor cells (Hession *et al.,* 1987; Sherblom *et al.,* 1988). Taking together, these data proposed that the lectin-like domain of TNF is spatially distinct from its receptor binding sites and is responsible for the TNF-mediated trypanolysis. Upon comparing the tertiary structures of TNF and lymphotoxin-α (LT-α) – a TNF homologous cytokine, able to bind to both the TNF receptors, lacking trypanolytic activity, the lectin-like domain of TNF was identified (Lucas *et al.,* 1994). The lectin-like domain encompasses the region of human TNF from S100 to E116 (S99 to E115 in murine TNF), which is located at the upper side of the pyramidal TNF shape, diametrically opposed to the receptor binding sites and found to be absent in both human and mouse LT-α (**Fig. 1**). This domain at the tip of the TNF molecule can be mimicked by a circular 17 amino acids peptide, named the **TIP peptide** (Lucas *et al.,* 1994). The TIP peptide was shown to exert trypanolytic activity, albeit at 10.000 times higher concentration, as compared to TNF (Lucas *et al.,* 1994). It was also shown that the TIP

peptide's amino acids T6, E8, and E11, but not P7 and G8 are crucial in mediating trypanolysis. The mutated TIP (mutTIP) peptide (T6A, E8A, and E11A) as well as scrambled TIP (scrTIP) peptide containing the same amino acids as the TIP peptide but in a random order were shown to be unable to mediate trypanolysis (Lucas *et al.,* 1994).

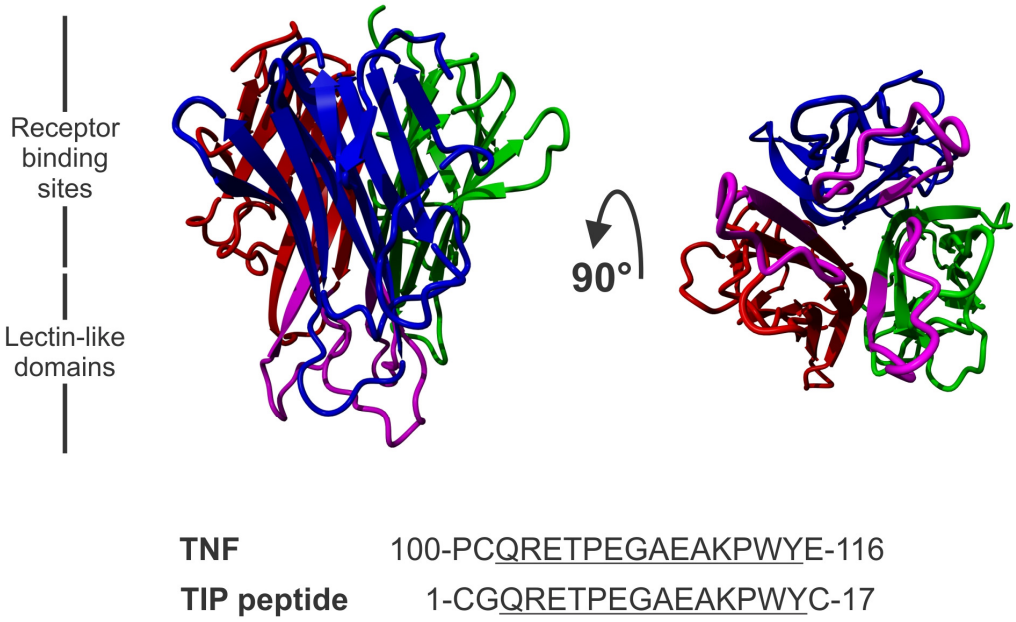

Figure 1. Top, ribbon representation of the TNF trimer (PDB code: 1TNF). Lectin-like domains are colored in magenta. **Bottom**, amino acid sequence of the lectin-like domain of the human TNF aligned with the sequence of the TIP peptide.

1.2.3 Structural features of peptides

One might think of peptides as rudimentary forms of proteins, and therefore playing less important role in nature. In order not to underestimate their value, I would like to illustrate few examples regarding the diversity of peptides and the role they play. Peptides are involved in many essential processes in signal transduction and cell-to-cell communications. Human peptide hormones like prolactin, vasopressin, oxytocin, and insulin, as well as several neuroactive peptides are essential players in the endocrine and central nervous systems. The number of synthetic peptides with novel biological functions is steadily and rapidly growing. These include enzyme and toxin inhibitors (Mourez *et al.,* 2001; Desjobert *et al.,* 2004), peptides with antiviral activity (Ho *et al.,* 2003; Sticht *et al.,* 2005), or peptides with the ability to specifically detect tissues with histological changes associated with diseases

(Wiesehan *et al.,* 2003; McGuire *et al.,* 2004). The TIP peptide was made cyclic, in order to retain as much as possible the initial structure of the lectin-like domain of the TNF it mimics. Cyclic peptides are not of unique structures, and already a number of cyclic peptides have been discovered in plants, bacteria, animals but not in humans, with sizes ranging from just a few to hundreds of amino acids in length (Craik 2006). Cyclic peptides can be classified according to the types of bonds that enclose the ring, and there are a number of cyclic peptide hormones which are cyclised through a disulfide bond between two cysteines, as in somatostatin and oxytocin. Cyclic peptides are also present among antibiotics (e.g. valinomycin, polymyxin B), immunosuppressive drugs (e.g. cyclosporine), and toxins (e.g. amanitin, microcystins). Some of the cyclic peptides like cyclotides, possess a broad variety of effects in cells, including anti-microbial, hemolytic, and anti-HIV activities (Craik *et al.,* 2004) and are still under study. Other cyclic peptides like octreotide (brand name Sandostatin™, Novartis) is already clinically approved and is used as a more potent analog of somatostatin for the treatment of acromegaly, diarrhea, and flushing (www.sandostatin.com). Upon cyclization, the TIP peptide has obtained a crucial property inherent to cyclic peptides – its stability (Antos *et al.,* 2009). Cyclic peptides tend to be extremely resistant to thermal and chemical denaturation and proteolysis, as compared to their linear analogs. Cyclic peptides are not targeted by exopeptidases – enzymes whose function is to digest the proteins (Craik 2006). This feature makes the cyclization process for both peptides and proteins very attractive for designers of protein- or peptide-based drugs (Scott *et al.,* 1999; Antos *et al.,* 2009; Popp *et al.,* 2011). Usually linear and even cyclic peptides possess flexible structures. The TIP peptide mimicking the loop structure of the lectin-like domain of TNF is not an exception here. Far-UV circular dichroism analysis of the secondary structure of the TIP peptide in physiological solution have shown that the TIP peptide adopts a random structure (van der Goot *et al.,* 1999). Attempts to solve the three-dimensional (3D) structure of the TIP peptide are described in **part 1.3** of this thesis, as well as in **publication III** attached to the thesis.

1.2.4 Therapeutically promising activities of the TIP peptide

The TIP peptide was shown to be trypanolytic; however, it later appeared to be not its only activity. Voltage-clamped whole-cell patch clamp experiments have shown that it increases outward currents in peritoneal macrophages, both outward and inward currents in primary lung microvascular endothelial (MVEC) cells both at acidic (6.0) and neutral (7.3) pH and mainly inward currents in airway epithelial cells (Hribar *et al.,* 1999; Hazemi *et al.,*

2010). Both analogs of the TIP peptide (mutTIP and scrTIP peptides) were shown to be inactive. This effect was blocked if the cells were pretreated with amiloride, an epithelial sodium channel (ENaC) blocker, showing direct or indirect effect of the TIP peptide on ENaC activation. It was hypothesized that the TIP peptide could act as an ion channel itself, explaining thus its membrane conductance in mammalian cells. This assumption was made because native TNF was proposed to interact with artificial lipid membranes possibly due to partial acidic unfolding and exposure of the hydrophobic residues (Hlodan and Pain 1994; Baldwin 1996). However, later experiments have not confirmed this, showing the inability of the TIP peptide to interact with liposomes (van der Goot *et al.,* 1999). These were the first results showing the capability of the TIP peptide to activate an amiloride-sensitive cationic channel in mammalian cells. Also, the idea of using the TIP peptide as a potent drug in resolution of alveolar fluid in patients with pulmonary edema was proposed for the first time.

Pulmonary edema is a life-threatening pathology which is characterized by accumulation of extravascular fluid in lungs, which can be accompanied by pulmonary endothelial and alveolar epithelial hyperpermeability (O'Brodovich 2005; Ware and Matthay 2005; Rimoldi *et al.,* 2009; Alwi 2010; Ford 2010; Murray 2011). This mostly occurs when the capacity of the alveoli to clear fluid in insufficient (Ware and Matthay 2005; O'Brodovich 2005). This will eventually lead to impaired gas exchange and may cause respiratory failure. Two fundamentally different types of pulmonary edema have been characterized: cardiogenic pulmonary edema (also termed hydrostatic or hemodynamic edema) and non-cardiogenic pulmonary edema (also known as permeability pulmonary edema), which occurs during acute lung injury (ALI), and the acute respiratory distress syndrome (ARDS) (Ware and Matthay 2005). Pulmonary edema can be caused by direct damage of the tissue or as a result of the heart or circulatory system malfunction. Alveolar epithelium (type 1 and type 2 cells) plays a primary role in the process of edema fluid clearance, which is based on the active transepithelial Na^+ transport via apical Na^+ channels (presumably by the ENaC) and the basolaterally located Na-K-ATPase with the water following iso-osmotically the Na^+ gradient (Matalon and O'Brodovich 1999; Matthay *et al.,* 2002; Mutlu and Sznajder 2005; Folkesson and Matthay 2006). Apart from ventilation strategies and β2-adrenergic agonists, no systematic treatments of pulmonary edema exist (Sakuma *et al.,* 1997; Modelska *et al.,* 1999), therefore the idea of using the TIP peptide to treat pulmonary edema, which, in contrast to β2-adrenergic agonists does not induce cAMP, holds promise (Lucas *et al.,* 2009).

Additional experiments with the TIP peptide further demonstrated its potential in resolving pulmonary edema. As such, the substance was shown to increase the lung liquid clearance (LLC) in the *in situ* mouse lung and the *ex vivo* isolated blood-perfused rat lung model, showing its potential physiological role in the resolution of pulmonary edema in rodents (Elia *et al.,* 2003). Since

the effects in both species were inhibited by amiloride, these results further indicate direct or indirect effects of the TIP peptide on ENaC.

The ability of the TIP peptide to activate LLC in a rat hydrostatic edema model *in vivo* was first reported in 2005 (Braun *et al.,* 2005). This study also showed that the disaccharide *N,N'*-diacetylchitobiose, previously reported to inhibit the TNF lectin-like activity as well as the TNF-mediated Na^+ transport (Hribar *et al.,* 1999), also inhibits the TIP peptide-mediated LLC activation. Therefore, these data suggested an important role of the lectin-like activity of the TIP peptide in its capacity to activate LLC.

The ability of the TIP peptide to interact directly with *N,N'*-diacetylchitobiose, but not with another disaccharide – cellobiose was demonstrated using high-resolution mass spectrometry (Marquardt *et al.,* 2007). This finding shed some light on the TIP peptide-carbohydrate interactions. What was also found is that cyclic and linear forms of the TIP peptide bind equally well to *N,N'*-diacetylchitobiose. However, the cyclic TIP peptide showed much higher stability for proteolytic degradation than the linearized one, which showed *N*-terminal degradation products. This was also supported by the fact that the cyclic TIP peptide has higher affinity to plasma proteins (like albumin and IgM) than the linear one. The mutant TIP peptide (mutTIP) had 30-40% less binding to *N,N'*-diacetylchitobiose, as compared to the native TIP peptide. This finding highlighted the important structure-function property of the TIP peptide; particularly, that the hexapeptide sequence TPEGAE represents only a partial binding motif for the lectin-like activity of the TIP peptide (Marquardt *et al.,* 2007). This is interesting, because the TIP peptide-carbohydrate interactions are also implicated in LLC mediated by the TIP peptide. The results of this study of the lectin-like domain-carbohydrate and TIP peptide-carbohydrate interactions are summarized in the **publication III**, attached to this thesis.

Until recently, all reported LLC activity of the TIP peptide was studied using the healthy, undamaged rodent lungs. However, liquid accumulation in lungs, is also a common consequence of ALI (Johnson and Matthay 2010) and ARDS syndrome (Matthay and Zemans 2011), which are usually accompanied by hyperpermeability of the alveolocapillary barrier. Recent studies have shown that the TIP peptide is also capable in preventing alveolar edema formation *ex vivo* in a rabbit model of hydrostatic edema by significantly reducing the hydrostatic pressure-induced increase in endothelial permeability (Vadász *et al.,* 2008). However, in this model the effect of the TIP peptide was almost identical to the effects of db-cAMP (analog of cAMP) administration, therefore questioning the clinical usage of the TIP peptide rather than cAMP enhancing agents. Nevertheless, the TIP peptide also significantly reduced capillary permeability and thus edema formation, after lungs were injured with *Staphylococcus aureus* α-toxin (exotoxin) and *Salmonella enterica*

lipopolysaccharide (endotoxin), the models in which vascular permeability was increased without elevating vascular pressure (Vadász *et al.,* 2008).

Recently, crucial discoveries were made regarding the potential of the TIP peptide to activate LLC and its structure-function relationships. Hamacher and colleagues highlighted the potency of the TIP peptide to improve lung function during ischemia reperfusion injury in a unilateral rat lung transplantation model of noncardiogenic ALI (Hamacher *et al.,* 2010). Significant increase in transplanted lung oxygenation as well as significant reduction of neutrophil infiltration in bronchoalveolar lavage was observed when the TIP peptide was added intratracheally. These beneficial effects were inhibited when animals were co-treated with the amiloride, or by pre-incubating of the TIP peptide with the *N,N'*-diacetylchitobiose. The TIP peptide was also shown to reduce hypoxia/reoxygenation-induced reactive oxygen species (ROS) generation in ovine pulmonary artery endothelial cells *in vitro* and to prevent ischemia reperfusion-induced ROS production in transplanted rat lungs *in vivo*. This finding is of great importance because of a lack of a specific treatment for ischemia reperfusion-mediated lung injury. Also, Ussing chamber experiments using a monolayer of primary rat alveolar type 2 epithelial cells showed that the primary receptor affected by the TIP peptide is located at the apical side of these cells, the place where the ENaC was shown to be localized (Renard *et al.,* 1995; Farman *et al.,* 1997), as such questioning the hypothesis that the primary target of the TIP peptide is the basolaterally located Na^+-K^+-ATPase (Vadász *et al.,* 2008).

Another recent work showed a protective property of the TIP peptide against bacterial toxin-induced hyperpermeability (Xiong *et al.,* 2010). *Listeria monocytogenes* by its major virulence factor listeriolysin (LLO) can cause listeriosis. In immunosuppressed individuals listeriosis can be accompanied by the pulmonary permeability edema. LLO, which is a cholesterol-binding pore-forming listerial exotoxin, increases endothelial permeability, initiated by Ca^{2+} influx, followed by protein kinase C (PKC) activation, ROS generation, RhoA activation and Rac1 inhibition, and myosin light chain phosphorylation (Repp *et al.,* 2002; van Nieuw Amerongen *et al.,* 2000; Birukova *et al.,* 2005; Xiong *et al.,* 2010). Permeability edema characterized by an extensive capillary endothelial hyperpermeability, requires immediate therapeutic treatment and often has a fatal outcome (Ananthraman *et al.,* 1983). However, there exists no standard therapy to treat pulmonary permeability edema yet. The TIP peptide was shown to blunt LLO-induced hyperpermeability *in vitro*, upon inhibiting PKC activation, ROS generation, myosin light chain phosphorylation and restoring RhoA/Rac1 balance; showing its potential in protecting from LLO-induced pulmonary endothelial hyperpermeability (Xiong *et al.,* 2010).

The same year essential TIP peptide features responsible for amiloride-sensitive Na^+ current activation in A549 cells were demonstrated and characterized (Hazemi *et al.,* 2010). Since it was already shown that ENaC is

directly or indirectly involved in the TIP peptide-mediated Na^+ uptake, this study focused primarily on structural properties of the TIP peptide responsible for this process. Cyclization of the TIP peptide introduced in order to retain the initial structure of the lectin-like domain of the TNF was done using of terminal cysteins with the subsequent disulfide bond formation upon oxidation. Reduction with the subsequent linearization of the peptide could eventually take place after administration of the TIP peptide, leading to less active (Lucas *et al.,* 1994) and less stable peptide (Marquardt *et al.,* 2007). Therefore, replacing weaker disulfide bond (bond distance ~2.05Å) by a stronger C-C or C-N bond (bond distance ~1.5Å) (Allen *et al.,* 1987) could potentially eliminate the above-mentioned disadvantages, also making the TIP peptide suitable for use as human medicine. Hazemi and colleagues described a series of novel cyclic peptides with several ways of NH- and COOH- coupling, and studied the effectiveness of those peptides in Na^+ current activation, using the patch clamp on the human lung epithelial cell line A549. Moreover, the selectivity of the TIP peptide activation effect on Na^+ over K^+ was investigated. Their major conclusions were that TIP peptide variants displaying ENaC-activating effect in A549 cells should possess: (i) a triad of residues equivalent to T105, E107, and E110 of human TNF, (ii) a group of adjacent hydrophobic residues equivalent to P113, W114, and Y115 of human TNF, and (iii) a positively charged N-terminal amino group, a negatively charged C-terminal carboxyl group or both of these, whereas peptides that lack one or more of these features do not exert such an effect (Hazemi *et al.,* 2010). All of the active TIP peptides were highly selective for the ENaC with a tendency to be less selective if a free positively charged N-terminal amino group was missing.

1.3 Aims of the thesis

Results from experimental studies described above suggest that the TNF-derived TIP peptide could represent a novel therapeutic avenue for the treatment of pulmonary edema. However, a lot of information concerning the mechanisms of the TIP peptide function is still missing. The aim of this thesis was to investigate the initial stages of the TIP peptide interaction with human lung epithelial cells (i.e. *in vitro*), and specifically with its putative receptor(s), studying the binding mechanisms on a molecular level. Various techniques, including single-molecular approaches, were used to this purpose. The study questions were the following:

1. The apical side of the lung epithelial cells was shown to be the target for the TIP peptide-mediated activity (Hamacher *et al.,* 2010). Biomolecules commonly act through interactions. Therefore, the first

question was: **Does the TIP peptide interact with the molecules located on the apical side of the lung epithelial cells?**

2. The existence of cell-penetrating peptides (Lundberg and Langel 2003; Prochiantz 2011), as well as peptides that function as vectors to deliver cargo bound to them were reported (Fischer *et al.,* 2001). The TIP peptide has a small molecular weight (M_r=1925) and a quarter of its residues are hydrophobic. Therefore, the second question was: **Does the TIP peptide need to be internalized inside of the cells to trigger its effects?**

3. Crucial amino acids as well as other structural features of the TIP peptide responsible for its activity were highlighted (Lucas *et al.,* 1994; Marquardt *et al.,* 2007; Hazemi *et al.,* 2010). However, the question remains: **What is the nature of the interaction between the TIP peptide and its putative receptor(s)?**

4. All previously reported results propose ENaC as a potential target for the TIP peptide. ENaC was shown to be activated upon binding small molecules (Ma *et al.,* 2007; Lu *et al.,* 2008), by various proteases (Kleyman *et al.,* 2009; Garcia-Caballero *et al.,* 2011; Svenningsen *et al.,* 2011), by methylation (Edinger *et al.,* 2006), by protein kinase Bα (Diakov *et al.,* 2010), and by shear stress (Fronius and Clauss 2008; Abi-Antoun *et al.,* 2011). Direct peptide binding to ENaC, however, followed by the inhibition of the channel was also reported (Ismailov *et al.,* 1999; Kashlan *et al.,* 2010). Therefore the important question remains: **What is the TIP peptide's receptor on the apical surface of the lung epithelial cells?**

Since the apical side of lung epithelial cells appeared to be a target for the TIP peptide, localization and visualization of the individual putative receptors becomes very important. Atomic force microscope (AFM) was used as an imaging device, due to its high resolution in visualizing live cells. However, the up-to-date imaging resolution of live cells under the AFM is usually around 20-100 nm, depending on the sharpness of the probes used and the particular cell and cell area being visualized (Butt *et al.,* 1990; Horber *et al.,* 1992; Le Grimellec *et al.,* 2000). The advantage of the higher harmonics (HH) AFM imaging in gaining better resolution, particularly in biological samples like bacteria and viruses, was reported (Preiner *et al.,* 2007; Turner *et al.,* 2009). For that reason, we have employed the HH AFM technique to resolve finer details of the live human H441 lung epithelial cell, as well as some other eukaryotic cells, with the results summarized in the **publication II** attached to this thesis. This was to our knowledge the only HH AFM imaging on

eukaryotic cells reported to date. Even though individual protein complexes on the surface of the lung epithelial cells were not resolved, better resolution compared to the conventional AFM techniques was observed. Also, correlation between the second harmonic amplitude and the stiffness of the various cell regions were discovered (**Fig. 2)**, and an eight times higher sensitivity of the second harmonic phase shift with respect to the first one was observed (**publication II**).

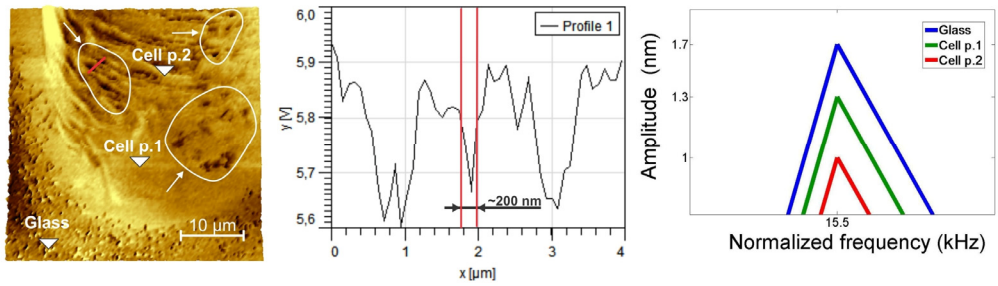

Figure 2. Left, second harmonic amplitude AFM image of human lung epithelial cell (H441), with extra features marked by white circles. **Middle**, the crossection profile of the cell's region marked by the red line on the AFM image. **Right**, frequency spectra recorded on a glass support, and two cell regions, highlighted on the AFM image. Curves are normalized to the main driving frequency.

To assess the possibility that the TIP peptide interacts with the apical side of lung epithelial cells, the single-molecule force spectroscopy (SMFS) technique was used. The TIP peptide, covalently attached to a flexible probe was brought in close contact with the apical surface of H441 cells, single TIP peptide-cell surface interactions were detected and the unbinding forces were measured. This method is extensively described in **chapter 2.2** of this thesis, and the results are summarized in **chapter 3**, and in the **publication IV** attached to this thesis.

In order to understand whether the TIP peptide is able to penetrate inside the cells to trigger its function, various approaches were used. For short peptides (~20–30 amino acids long) that are not folded, several physicochemical properties can be estimated using the sum of the values of the isolated residues present in the peptides. If we look at such properties like a charge of the peptide at physiological pH (7.4) and a hydropathy index (Kyte and Doolittle 1982) – a measure of the hydrophobicity, we can conclude that a low amount of hydrophobic amino acids (4 out of 17), and a negative sum of the hydropathy index of the TIP peptide's amino acids (−20.7) define it as a hydrophilic molecule. At physiological pH, the net charge of the TIP peptide appears to be negative, just like the surface charge of the cells. Both of these

assumptions therefore suggest that passive interaction with the cell membrane and internalization of the TIP peptide is highly unlikely.

Peptide vectors capable of transporting molecules into cells in the form of covalent conjugates by energetically-independent mechanism were reported (reviewed in Fischer *et al.,* 2001). No sequence homology was observed between these peptide vectors, but only general features such as charge distribution and hydrophobicity seem to be common.

	charge at 7.4[1)]	**hydropathy index**	**number of amino acids**
TIP peptide	-1.3	-20.7	17
delivery peptide vectors*			
pAntp(43-58); Penetratin	6.8	-27.7	16
retro-inverso pAntp(43-58)	6.8	-28.3	16
W/R Penetratin	9.8	-50.4	16
pAntp(52-58)	4.8	-19.7	7
HIV TAT	7.8	-45.4	13
HIV TAT2	7.8	-40	11
r7	6.8	-31.5	7
gp41 fusion sequence	-0.2	18.9	17
MPG (gp41fusion sequence - SV40 NLS)	3.8	3	27
Caiman crocodylus Ig(v) light chain	-0.1	28.2	17
Caiman crocodylus Ig(v) light chain - SV40 NLS	4.9	5.5	27
PreS2-TLM	-0.2	1.6	12
Transportan	3.8	17.1	27
SynB1	5.8	-27.5	18
MPS (kaposi FGF signal sequence)	-0.2	38.8	16
MPS (kaposi FGF signal sequence) 2	-0.2	27.6	12
MPS (human integrin β_3 signal sequence)	-0.2	31.3	15
P3	5.8	-27.6	30
Model amphiphilic peptide	4.8	17.9	18
KALA	4.8	8.5	30

Table 1. Comparison of the charges and hydropathy indexes of the TIP peptide and delivery peptide vectors (* described in Fischer *et al.,* 2001). [1)] calculated using Protein Calculator v3.3 at: www.scripps.edu/~cdputnam/protcalc.html

Perhaps, if the TIP peptide has the same physicochemical properties as the delivery peptide vectors, it might use the same mechanism to enter the cells? If we look at the charge and the hydropathy index of some of the peptide vectors, and compare them with that of the TIP peptide (**Table 1**), we can observe that: (i) most of the delivery peptides (70%) possess a positive charge, (ii) those that have negative charge (not lower then –0.2) have a positive (usually >20) hydropathy index, and (iii) none of them have both negative charge and

negative hydropathy index, like the TIP peptide does. Therefore, comparison of the charge and hydropathy indexes of the 20 delivery peptides with that of the TIP peptide indicates that the TIP peptide does not have the physicochemical properties of the delivery peptides, and therefore cannot possess their membrane penetration activity.

Another manner to investigate whether the TIP peptide could penetrate the cells was done using direct labeling of the TIP peptide with a fluorescent dye. The amino-reactive dye (Atto 465 NHS ester, *Fluka*) was covalently attached to the TIP peptide resulting in a small high-sensitive fluorescent probe. The fluorescently labeled TIP peptide was incubated with the H441 cells for 30 minutes. Afterwards, the cells were washed to remove unbound probe and analyzed using laser-scanning confocal microscope. The fluorescent signal of the labeled TIP peptide was localized in the plasma membrane of the cells but not in the cell's interior (**Fig. 3**). To verify that the TIP peptide properties are not affected by attachment of the fluorophore, the fluorescently labeled TIP peptide was tested to activate transepithelial current in the confluent monolayer of the H441 cells using Ussing chamber (Ussing and Zerahn 1951). Fluorescently labeled TIP peptide was able to mediate transepithelial current in the culture of the H441 cells to the same degree as a native one (**Fig. 4**).

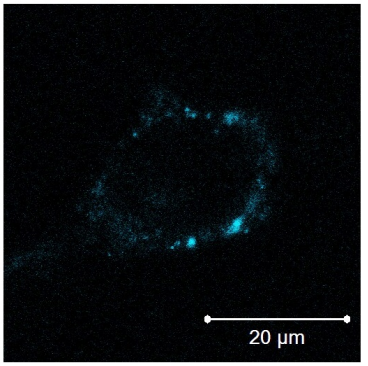

Figure 3. Confocal image of the H441 cell labeled with the Atto-NHS-TIP peptide probe.

Search for the TIP peptide's still unknown receptor(s) and understanding the interaction mechanism between them represents a big challenge. However, the TIP peptide possesses several features that potentially narrow our investigation to membrane bound glycosylated receptors only. First, the TIP peptide mimics the lectin-like domain of the TNF which has affinity to sugars, like *N,N'*-diacetylchitobiose and branched trimannoses. Second, the activity of the TIP peptide was shown to be blocked by its preincubation with the *N,N'*-diacetylchitobiose but not cellobiose. Hence, the TIP peptide-carbohydrate interactions were prioritized also in light of the fact that ENaC possesses several glycosylation sites (Canessa *et al.,* 1994; Voilley *et al.,* 1994;

Kleyman *et al.,* 2009). When probing the interaction mechanisms, the knowledge of the 3D structures of the ligand and the receptor is a must. In order to obtain 3D structure of the TIP peptide, two very different approaches were used: a computational one – structural modeling, and an experimental one – a macromolecular crystallization together with the X-ray diffraction analysis. Using the computational method and known 3D structure of human TNF (PDB code: 1TNF), a model of the TIP peptide resembling the structure of the lectin-like domain was built. The structure of the TIP peptide was further used for molecular docking and molecular dynamics simulation (methods described in **chapters 2.3** and **2.4**) with the oligosaccharides *N,N'*-diacetylchitobiose, trimannose-*O*-ethyl, and cellobiose. The results of this work are summarized in **chapter 3**, and in the **publication III** attached to this thesis.

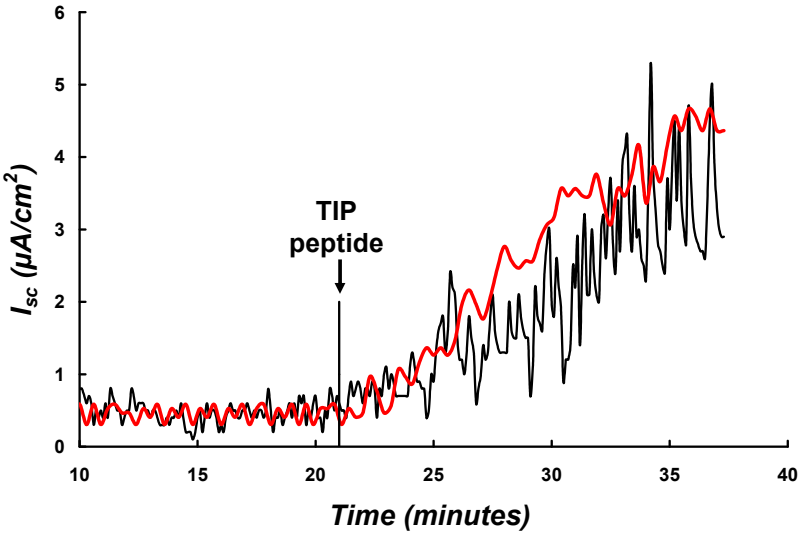

Figure 4. Short circuit current (I_{sc}) of the epithelial cells (H441) monolayer in Ussing chamber. Stimulation the apical side of the cells with the fluorescently labeled TIP peptide (2.5 μg, vertical line) results in continues increase of the I_{sc} (black line), to the same degree as a native TIP peptide (red line). (Measurements were done at the University of the Applied Sciences in Krems, Austria by Mag. Maren Pflüger).

Unfortunately, computer-built models often require further verification using experimental techniques. X-ray crystallography, together with the NMR spectroscopy are two major structure resolving methods, which provide highly reliable results. High concentrated solution of the chemically synthesized TIP peptide was crystallized and the large enough crystals suitable for further X-ray diffraction analysis were obtained (**Fig. 5, left**). Interestingly, the TIP peptide crystals grew along with the crystals of the precipitant, and were differentiated using the crush test and dye absorption methods. Obtaining high quality crystals

is an important prerequisite for X-ray crystallography which however does not guarantee their diffraction. Unfortunately, diffraction pictures of the TIP peptide crystals were unsuitable for further structure determination (**Fig. 5, right**).

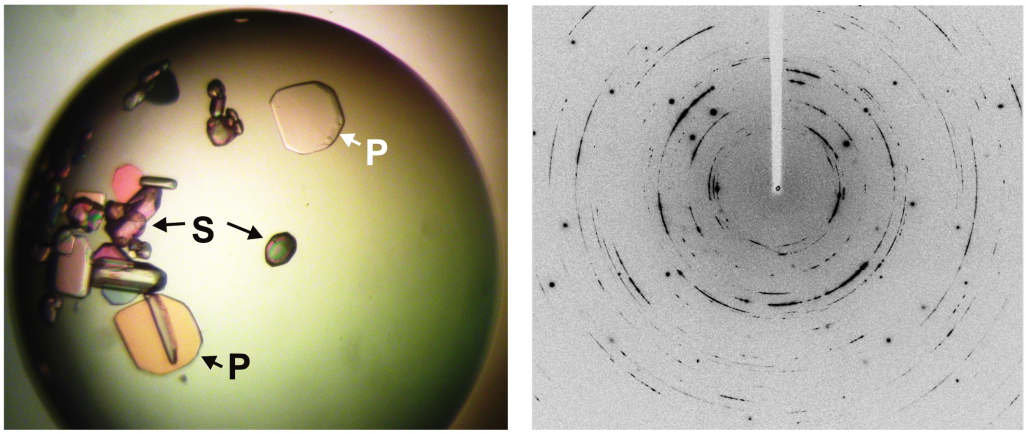

Figure 5. **Left**, crystallization drop with the TIP peptide (P) and salt (S) crystals growing using sitting drop vapor-diffusion method at 22 °C. The drop contains 2 µL of 100 mg/ml TIP peptide water solution with 2 µL reservoir solution composed of 0.1 M HEPES, 0.6 M potassium sodium tartrate tetrahydrate, pH=7.5. **Right**, the X-ray diffraction image of the TIP peptide crystal obtained at BESSY II beamline 14.1 in Berlin, Germany.

The specific interactions between the TIP peptide and the apical surface of the lung epithelial cells have been observed and measured using the SMFS technique. This method however does not provide any information regarding the identity of the binding partner for the TIP peptide. To answer this, perhaps the most challenging question, the molecular biological methods were utilized. The TIP peptide was immobilized on the NHS-Sepharose (*GE Healthcare*) using the amino group of the TIP peptide's only lysine residue. The plasma membranes from the H441 cells were isolated and membrane proteins were solubilized using 0.1% (w/w) *n*-Dodecyl-*β*-maltoside (*SIGMA*). Membrane proteins were then applied onto the TIP peptide-functionalized Sepharose column, and those unable to interact with the TIP peptide were washed. Bound to the TIP peptide proteins were eluted with the 1 M NaCl containing buffer, concentrated, and separated using the 10% SDS-PAGE. Eleven protein bands with the mass ranging between 37 kDa to 110 kDa were identified (**Fig. 6**). According to the mass comparison, three out of 11 proteins were probably present in a dimer form, therefore resulting in the presence of only eight unique proteins. Possibly, the number of the unique binding partners to the TIP peptide could be even lower due to the fact that some of these bands could be degradation products. Four major bands (# 1, 2, 4, and 5), having the highest protein content were sent for mass spectrometry identification. Unfortunately,

the identification failed due to the insufficient amount of the proteins in the samples.

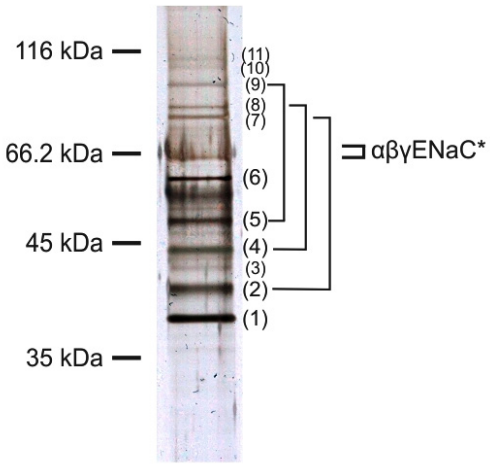

Figure 6. Silver stained 10% SDS-PAGE of the eluted proteins bound to the TIP-Sepharose. Numbers in brackets correspond to the distinguished protein bands, and the possible dimers with the corresponding monomers are interconnected by lines. * Approximate localization of the ENaC subunits (α, β, and γ) according to Canessa *et al.* 1994.

Chapter 2

Materials and Methods

To gain understanding of the TIP peptide action, various biophysical and biochemical methods were utilized. Atomic force microscopy technique allowed us to visualize the primary target of the TIP peptide – surface of the lung epithelial cells at high resolution. Using single-molecule force spectroscopy, binding between the TIP peptide and the cell surface was probed and the binding forces were measured down to a piconewton range. Molecular docking and molecular dynamics simulations methods allowed us to find most probable binding site for *N,N'*-diacetylchitobiose, identify the amino acids involved and characterize such interactions. Search for the potential TIP peptide binding partners was done using techniques of molecular biology and mass spectrometry. Many other common techniques and methods were used on a regular basis.

2.1 Scanning probe microscopy

Scanning probe microscopy (SPM) is absolutely unique branch of microscopy since no matter (photons or electrons) transmission or dispersion through the sample is taking place. The topographical image of the surface is formed by a physical probe that scans the specimen by mechanical line by line movements – raster scans. The image down to atomic level represents various probe-surface interactions as a function of position. Such unprecedented resolution coupled with the ability to operate at ambient conditions made the SPM one of the most celebrated instruments not only in biological sciences.

2.1.1 The history of SPM

Traditionally, the advent of the SPM is referred to 1981, when the scanning tunneling microscope (STM) was introduced by Binnig and Rohrer at IBM Zurich Research Laboratory. Their milestone results: principle of STM and topographic pictures of $CaIrSn_4$ and Au surfaces on an atomic scale, were published the following year (Binnig *et al.,* 1982). The story of SPM however started back in 1928, when E.H. Synge proposed a theoretical design of an optical imaging device using sharp glass tip scanned across the sample in a near proximity to prevent light from lateral dispersion (Synge 1928). Four years later he had also proposed to use piezoelectric actuators with the scanning microscope (Synge 1932), exactly as it was developed 50 years later. In 1929 G. Schmalz builds the stylus profiler that had a sharp tip at the end of a cantilever in perpetual contact with the sample, and optical movement detection technique (Schmalz 1929). It is interesting to mention that Edison's phonograph

for playing sound recordings was almost 30 years on a mass market already, being slowly replaced by the radio. The next mentioning of the "probe microscopy" is dated to post World War II period. In 1955 an US Patent #2728222 was issued to Helmut Becker and others for their invention of "Apparatus for measuring surface irregularities". Their invention featured an oscillation probe to provide intermittent contact between the stylus and sample, and a method to measure the amplitude of the probe as a measure of the sample topography. In this work the first attempts to provide drawbacks of the contact mode stylus profiling were proposed. Next year, in 1956 O'Keefe reinvents the theoretical scanning principle proposed by E.H. Synge (O'Keefe 1956), and A.V. Baez verified experimentally the concept of near field scanning (Baez 1956). Another breakthrough was done in 1972, when R. Young, J. Ward, and F. Scire introduced the Topografiner – a non-contact scanning probe instrument that relies on electric field emission and metal-vacuum-metal tunneling for mapping and measuring the microtopography of hard surfaces (Young *et al.,* 1972). They were able to achieve 3 nm vertical and 400 nm lateral resolutions, however failed in utilizing the tunneling effect due to excess vibrations. This instrument already has many of the main components of a modern scanning tunneling microscope, that was introduced in less then 10 years. The 1982 paper of Binnig and colleagues in the Physical Review Letters named "Surface Studies by Scanning Tunneling Microscopy" starts the era of scanning tunneling microscopy – a primary SPM mode (Binnig *et al.,* 1982). Their first STM was constructed in IBM Zurich research laboratory in Switzerland, was operated in vacuum using piezoceramics feedback, and vibrations were damped by magnetic levitation. The same year, another discovery at the IBM Zurich research laboratory was done. Scanning Near-Field Optical Microscope, also known as SNOM, showing sub-wavelength (optical) resolution (25 nm) at visible wavelength using near-field optical techniques. The first results were published 2 years later in a paper entitled: "Optical stethoscopy: image recording with resolution λ/2" (Pohl *et al.,* 1984). A year after that, Gerd Binnig and Calvin F. Quate in Edward L. Ginzton laboratory at Stanford University together with Ch. Gerber at San Jose IBM research laboratory invented the atomic force microscope (AFM) – perhaps the most widely used SPM. Their paper in 1986 issue of Physical Review Letters (Binnig *et al.,* 1986) have been cited 7,063 times (as of December 5, 2011 from Web of Science). Apparently, 1986 was epochal year for the SPM in general. On April 4, 1986 the cover page of Science journal featured atomic surface of a silicon crystal obtained from a STM – the first SPM image to appear on the cover of a journal. The same year two sub-modes of SPM were introduced: Scanning Thermal Microscope (SThM) (Williams and Wickramasinghe 1986) and Magnetic Force Microscope (results were published the following year (Martin and Wickramasinghe 1987; Saenz *et al.,* 1987).

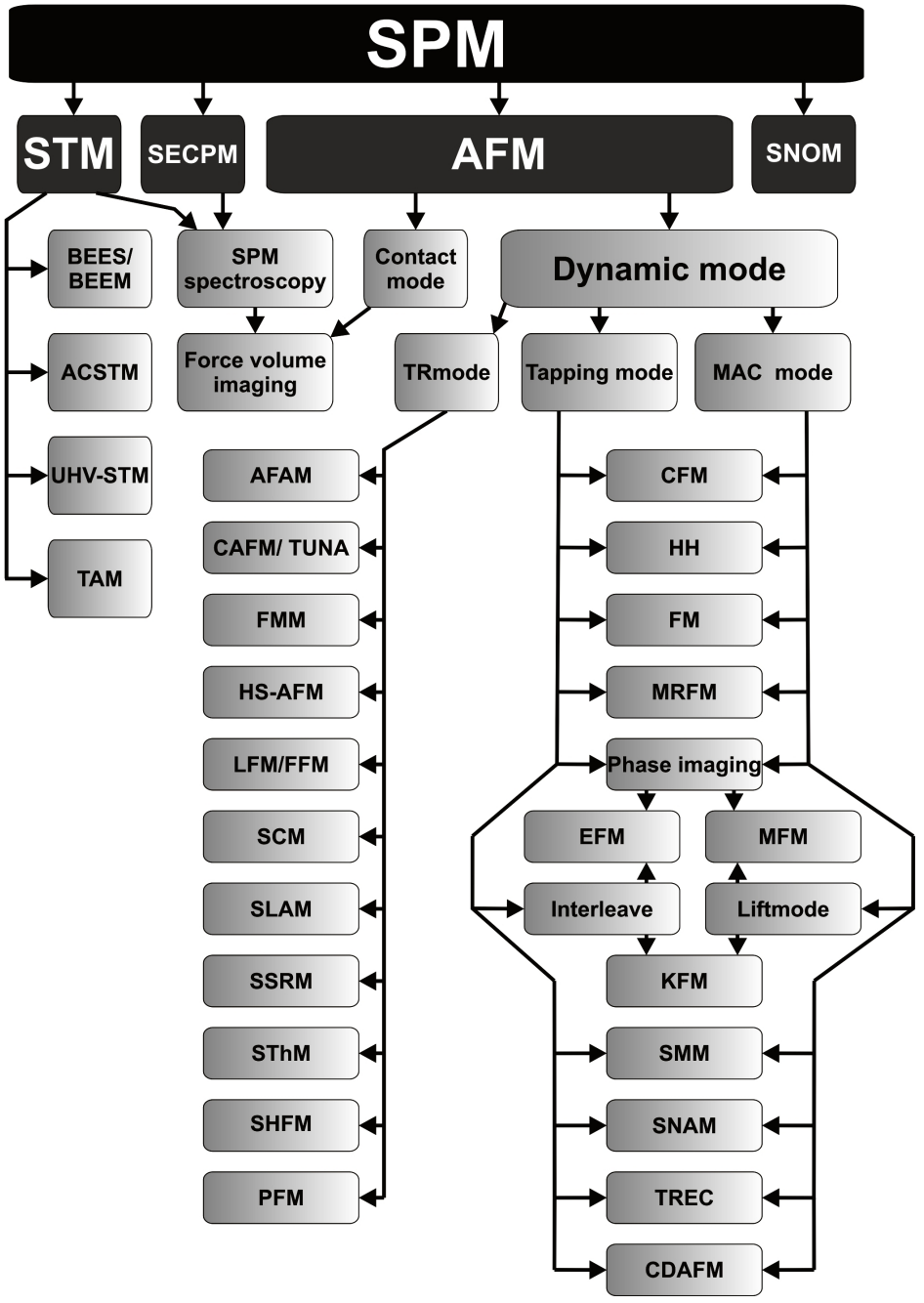

Figure 7. The variety of SPM (not a full list). SPM – scanning probe microscopy, STM – scanning tunneling microscopy, SECPM – scanning electrochemical potential microscopy, AFM – atomic force microscopy, SNOM – scanning near-field optical microscopy, BEES/BEEM – ballistic electron emission spectroscopy/microscopy, ACSTM – alternating current scanning tunneling microscopy, UHV-STM – ultra-high vacuum scanning tunneling microscopy, TAM – tunneling acoustic microscopy, TRmode – torsion resonance mode, MAC

mode – magnetically actuated mode, AFAM – atomic force acoustic microscopy, CAFM – conductance AFM, FMM – force modulation microscopy, HS-AFM – high speed AFM, LFM – lateral force microscopy, FFM – friction force microscopy, SCM – scanning capacitance microscopy, SLAM – scanning local-acceleration microscopy, SSRM – scanning spreading resistance microscopy, SThM – scanning thermal microscopy, SHFM – shear-force microscopy, PFM – piezoresponse microscopy, CFM – chemical force microscopy, HH – higher harmonics imaging, FM – frequency modulation microscopy, MRFM – magnetic resonance force microscopy, EFM – electric force microscopy, MFM – magnetic force microscopy, KFM – Kelvin force microscopy, SMM – scanning Maxwell-stress microscopy, SNAM – scanning near-field acoustic microscopy, TREC – topography and recognition imaging, CDAFM – critical dimension atomic force microscopy.

By that time, SPM and STM particularly has proved to be the powerful self-standing method for surface characterization on atomic level that was awarded by the Nobel Prize committee in 1986. The subsequent years until the end of the 20th century were the years of evolution of the SPM. The new sub-type of scanning probe microscopy was emerging almost every year. To keep it short, I will just mention the major achievements in the order of appearance. In 1987 the non-contact (attractive mode) AFM (Martin *et al.,* 1987), magnetic STM (Allenspach *et al.,* 1987) and lateral (friction) force microscope (Mate *et al.,* 1987) were introduced. The same year atomic-scale manipulation of individual atoms from an STM probe to a substrate was reported for the first time (Becker *et al.,* 1987). In 1988 the electrostatic force microscope was introduced (Martin *et al.,* 1988). During the year 1989 invention of scanning spin-precision microscope (Manassen *et al.,* 1989) and scanning electrochemical microscope (Husser *et al.,* 1989) were reported. The same year observations of the sample damage imposed by the scanning process led to use of AFM as a nanolithography tool. In 1990 scientists from IBM successfully arranged atom-by-atom 37 Xeon atoms on a single-crystal substrate using STM operating at 4 Kelvin, producing the smallest IBM writing in a history (Eigler and Schweizer 1990). Same year STM was utilized in nano-chemical modification of hydrogen-passivated silicon by scanning in air (Dagata *et al.,* 1990). In 1991 force modulation AFM (Maivald *et al.,* 1991) and Kelvin probe microscope (Nonnenmacher *et al.,* 1991) were introduced. In 1992 TappingMode™ AFM was introduced by Digital Instruments Company (now a part of Bruker scientific instruments division) with the US Patent #5412980 assigned in 1995. In 1993 piezoresponse microscopy using tunneling microscopy was introduced, with the result published following year (Franke *et al.,* 1994; Takata *et al.,* 1994). In 1995 Franz J. Giessibl reported atomic resolution of the Silicon (111)-(7×7) surface using non-contact AFM in ultrahigh vacuum, achieving unprecedented 6 angstroms lateral and 0.1 angstrom vertical resolution (Giessibl 1995). In 1996 three major SPM events have been reported: (i) magnetically actuated cantilever mode (MACmode™) AFM is reported by Han and Lindsay (Han *et al.,* 1996) from Molecular Imaging Corporation (today Agilent Technologies); (ii) dynamic friction force microscopy is introduced,

using lateral dither of the AFM tip (Colchero *et al.,* 1996); and (iii) for the first time carbon nanotube attached to AFM and STM probes were used for imaging (Dai *et al.,* 1996). In 1997-1999 the important works in nanofabrication, nanoshaping, and dip-pen nanolithography were done (Xu and Liu 1997; Piner *et al.,* 1999). Also in 1999 a combination of dynamic force microscopy with the simultaneous molecular recognition imaging was introduced (Raab et al., 1999). The method is now commercially available as PicoTREC™ from Agilent Technologies. In 2002 torsional resonance mode AFM was developed in both non-contact and contact regimes (Kawagishi *et al.,* 2002; Pfeiffer *et al.,* 2002).

2.1.2 The principle of SPMs

The SPM uses a micro-actuator, the scanner that positions the probe respective to the sample either by moving a probe (a sharp tip) or a sample. The interactions between the probe and a sample are sensed by a detector or a sensor. SPM utilizes feedback loop to control the strength and polarity of SPM probe-sample interactions with the user defined setpoint value. The instantaneous difference between a feedback loop's setpoint and input signal is its **error signal**. SPM data is usually **detector signal**, **sensor signal**, **error signal**, or **output signal** values, mapped or plotted against the coordinates X, Y, Z, or against a ramped parameter, such as a voltage applied to a probe or a sample. SPM raster-scans the probe or sample in XY plane to create 3-dimensional images.

AFM is the most widely used form of SPM, since it requires neither an electrically conductive sample, as in STM, nor an optically transparent sample or substrate, as in most SNOMs. Since the AFM was the only SPM utilized in this thesis, the principle of AFM will be explained in more details here.

The working principle of AFM is the following. A sharp probe (or tip) with an apex of a few nanometers on the outer end of a flexible cantilever is brought into contact with the sample surface. Afterwards, the probe or the sample is laterally moved over the surface and the cantilever deflection is measured (**Fig. 8, left**). This could be accomplished by different ways: by placing an STM tip above cantilever and monitor tunneling current; by monitoring focused laser beam reflection; by measuring capacitance between the cantilever and above located conductor or through a piezoelectric layer on the cantilever that registers a voltage upon deflection. Nowadays, all commercially available AFMs use focused laser beam reflection to monitor cantilever deflection. Minuscule changes of the cantilever deflection are magnified by an optical lever and recorded by a 2 or 4 segment photodiode detector. The relative position between the scanning probe and the sample surface is controlled by a piezo scanner. An electric field applied to a piezo

causes changes in the crystal structure and thereby a contraction or expansion of the scanner, allowing movements with sub-nanometer accuracy. This simple and effective operating principle allows obtaining a lateral resolution in the range of five to ten angstroms, and a vertical resolution of one to two angstroms.

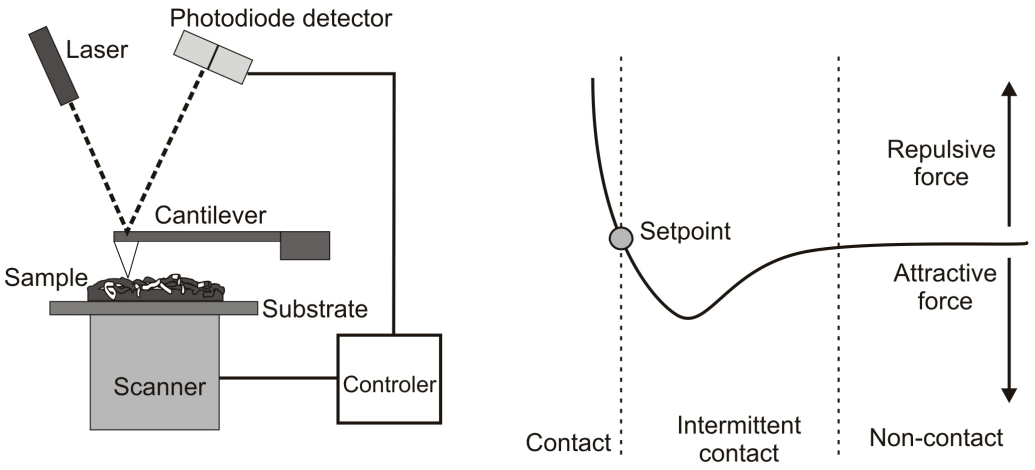

Figure 8. **Left**, schematic principle of AFM. The visualized sample is deposited on atomically flat substrate surface which is coupled to the AFM scanner which enables its movements with the sub-nanometer ranges. Atomically sharp AFM tip which is located on the apex of the flexible cantilever probing the surface causing the cantilever to bend. Bending of the cantilever is detected upon changes in the laser beam reflection from its opposite surface with the laser spot detected by a photodiode detector. The controller which is operated by a computer, interconnects together all the AFM parts. **Right**, force-distance plot, representing the forces acting between an AFM probe and a sample. When a probe and a sample are brought close to each other they start to sense surface forces arising from various interactions (van der Waals, electrostatic, hydration, etc.) between them. This is a *non-contact* region. While AFM operates in dynamic mode (e.g. Tapping or MAC, see text), the interactions usually take place in the *intermittent* contact region. Finally, the region where probe touches the sample is called *contact* region.

In static AFM operation modes, the force acting on the cantilever is directly translated into the deflection. Here the cantilever deflection (and thereby the force) is held constant by the compensating motion of the z-piezo. An important parameter defining probe-surface interactions (except the tip aperture) is the cantilever spring constant.

The applied force to soft samples can easily exceed a critical value, especially with hard cantilevers having a high spring constants. Therefore a variety of silicon and silicon nitride (Si_3N_4) cantilevers with spring constants ranging from 0.01 to 100 N/m, and resonant frequencies ranging from 5 kHz to over 300 kHz are used. There are two basic structural designs for the AFM cantilevers: straight rectangular and V-shaped (triangular). The cantilever

carrying the tip is attached to a small glass chip enabling easy handling and manipulation (**Fig. 9**). The probe (or a tip), which is located at the end of the cantilever is a key element of AFM since it determines its spatial resolution. AFM tip is the only part which is in direct contact with a sample and takes part in formation of an image through their force interactions. Usually the tip is a 3 μm tall pyramid with 2-30 nm end radius. The essential tip parameters are the radius of curvature and an aspect ratio. It is very important that the tip apex is sharp and tall enough compared to the object to be visualized. Electron-beam-induced coating of the tips could drastically improve their aspect ratio, although with the drawback of fragility. Carbon nanotubes that have one-dimensional tube structure, small diameter, high-aspect ratio and high stiffness were successfully utilized in fabricating the AFM probes (Dai *et al.,* 1996; Gibson *et al.,* 2007).

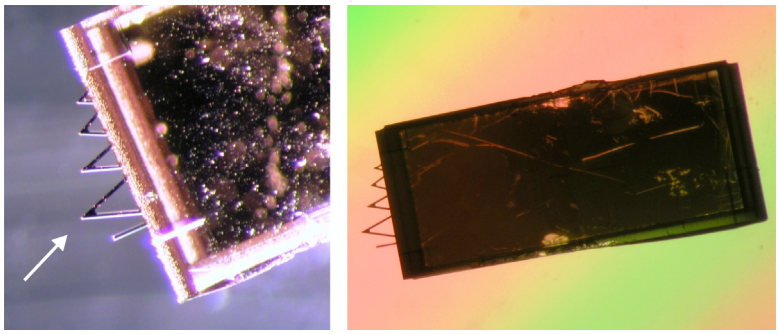

Figure 9. Image of the silicone nitride AFM chip with cantilevers (MSCT, *Bruker*). The largest triangular cantilever (white arrow) with length 310 μm, width 20 μm, and thickness 0.55 μm was used for contact mode imaging and SMFS experiments done in this thesis.

In dynamic AFM operation modes (tapping and MAC), the problem of probe-induced damage of a sample is largely overcome. Here the cantilever oscillation is driven by acoustic (tapping mode) or magnetic (MAC mode) forcing. In the amplitude modulation mode a fixed excitation frequency close to the resonance frequency is used. Changes of the oscillation amplitude reveal topographical changes in the image. In frequency-modulated dynamic AFM imaging, the resonance-frequency is used to drive the feedback loop.

A substrate surface, on which a sample is placed, plays an important role in AFM imaging. It should be flat enough so that object of interest deposited on it could be easily identified. Also, it should be clean and free as possible of any defects that may turn out as artifacts in the images. Among the widely used imaging surfaces are: mica, graphite, and gold surfaces.

- Mica – freshly cleaved muscovite mica has a perfectly pure and atomically flat surface, therefore, ideally suited as an AFM

substrate. Mica has got strong negative charge, leading to a very tight electrostatic binding of various biomolecules. Negatively charged molecules (e.g. nucleic acids) can also be firmly bound to mica through mediatory divalent cations such as Zn^{2+}, Ni^{2+} or Mg^{2+}.

- Graphite – highly ordered pyrolytic graphite or highly oriented pyrolytic graphite (HOPG) has atomically flat hydrophobic surface which is easily renewable by cleaving. The distance between carbon atoms in HOPG is used for STM and AFM calibration.
- Gold surfaces – are excellent substrates, because they do not have surface oxide and remain clean for a long period of time. They are also easily cleaned and therefore reusable.

2.1.3 Interaction forces between the AFM probe and a sample

The AFM probe-sample interactions are complex and comprise of various forces, depending on microscopy mode used and the environment (air or liquid) (**Fig. 10**). The **Electrostatic**, or **Coulombic**, **force** is by far the strongest force within intermolecular interactions. In the most AFM operation modes however, the AFM probe and a sample are not charged, allowing this force to be ignored. The **van der Waals force** plays important role in probe-sample interactions, also because it is present in electrically neutral materials. The van der Waals force acting between the probe and a sample is the sum of three different forces, all proportional to $1/r^6$ (where r is the distance between the atoms or molecules) (Cappella and Dietler 1999):

1. The orientation or **Keesom force** – is the angle-averaged dipole-dipole interaction between two atoms or molecules.

2. The induction or **Debye force** – is the angle-averaged dipole-induced dipole interaction between two atoms or molecules.

3. The dispersion or **London force** – is the major contributor to van der Waals force, since it acts between all molecules or atoms, on a distances ranging between 10 and 0.2 nm. This force could be both attractive and repulsive, and represents instantaneous dipole-induced dipole interaction, and is of quantum mechanical nature.

During the in air operation of the AFM, the probe contacts the surface of the liquid film that usually covers the sample. Thus the meniscus of liquid is

formed, resulting in attractive **capillary force** generation. It can be eliminated either by removing the water layer (dry environment or vacuum), or by dipping both probe and a sample into a liquid environment. It was shown that the capillary force, and hence the total adhesion force diminishes when the probe is coated with the hydrophobic material (Eastman and Zhu 1996).

When imaging in aqueous media, and mica is used as a substrate, it can attract oppositely charged ions from the solution leading them to cluster at the solid-liquid interface forming a positively charged layer. The **electrostatic repulsion** will be therefore exerted to an AFM probe. It can be overcame by increasing the ionic strength of the imaging media by adding a small quantity (a few mM) of a salt containing divalent metal ions (Morris *et al.,* 2010).

Among the other forces that could influence the probe-sample interactions are: Casimir forces, hydrophobic forces, steric forces, solvation forces, etc.

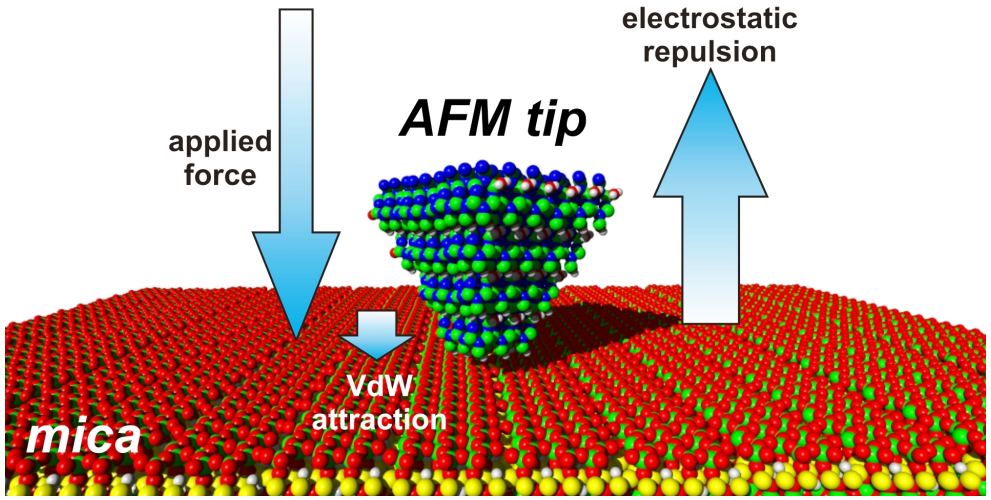

Figure 10. Representation of the forces acting between the silicone nitride probe and mica surface.

2.2 Single-molecule force spectroscopy

The AFM-based single-molecular force spectroscopy (SMFS) is a form of SPM spectroscopy (Hinterdorfer *et al.,* 1996; Kienberger *et al.,* 2006) where a ligand-functionalized probe is repeatedly brought into contact with the sample surface, containing the corresponding receptor. Thus a ligand and a receptor may form a complex, and the forced dissociation process is followed over time. In addition, dynamical aspects regarding the recognition process are addressed by applying different loading rates, yielding characteristic force-time profile.

The latter provides information about the unbinding kinetics as well as about the energy landscape. To compare with the traditionally bulk measurements, SMFS is a single-molecule technique, meaning there is no averaging over the whole ensemble of molecules present in a sample. SMFS intends to probe weak non-covalent interactions such as: hydrogen bonds, hydrophobic and electrostatic interactions.

2.2.1 Probe and surface chemistry

SMFS, as well as TREC, are based on a ligand-functionalized probe and receptor functionalized surface. Therefore, stable (usually covalent) attachment of both binding partners, are of a key importance. The most common steps of probe functionalization are the following: (i) aminofunctionalization, (ii) binding of the distensible crosslinker, and (iii) attachment of the specific ligand.

Aminofunctionalization

The general way to introduce reactive sites on initially inert probe materials like silicone or silicon nitride is the aminofunctionalization (Hinterdorfer *et al.,* 1996; Chowdhury and Luckham 1998; Riener *et al.,* 2003; Ebner *et al.,* 2007). Since this step affects the final concentration of the ligands on the probe surface, all methods used have to fulfill the requirement, that in the end only one or very few ligands are bound to the apex of the probe. In addition, the surface should not get sticky; otherwise unspecific adhesion will interfere with specific interactions. One of the strategies for aminofunctionalization of the silicon and silicone nitride probes is the liquid phase reaction with ethanolamine hydrochloride (Hinterdorfer *et al.,* 1996; Riener *et al.,* 2003).

Binding of the distensible crosslinker

After the generation of reactive sites, i.e. amino groups, the next step is the covalent binding of a heterobifunctional crosslinker. Homobifunctional linkers are used rarely since they can form loops. The chemical and physical property of the linker is of key importance for successful single-molecule experiment. Linear polymers, such as carboxymethylamylose, poly-(*N*-succinimidyl acrylate), or polyethylene glycol (PEG) chains have been successfully used as flexible tethers linking the molecules to the AFM probes. PEG for instance is a water soluble and nontoxic polymer which is used in a broad range of applications. Its major advantages are the protein repelling property (Ebner *et al.,* 2004) and elastic behavior (Kienberger *et al.,* 2000). PEG stretching during the measurements is a purely elastic (and therefore totally reversible) process. From the chemical point of view, PEG is chemically

stable, available in required chain-length, and soluble in all relevant solvents like chloroform and water. For these reasons, PEG linkers have been successfully utilized in a majority of SMFS and TREC experiments (Hinterdorfer *et al.,* 1996; Kienberger *et al.,* 2000; Nevo *et al.,* 2003; Riener *et al.,* 2003; Kienberger *et al.,* 2006; Chtcheglova *et al.,* 2007; Puntheeranurak *et al.,* 2007). Nearly all crosslinkers for amino-reactive probes are coupled via an activated carboxylic acid, usually N-hydroxysuccinimide ester (NHS ester).

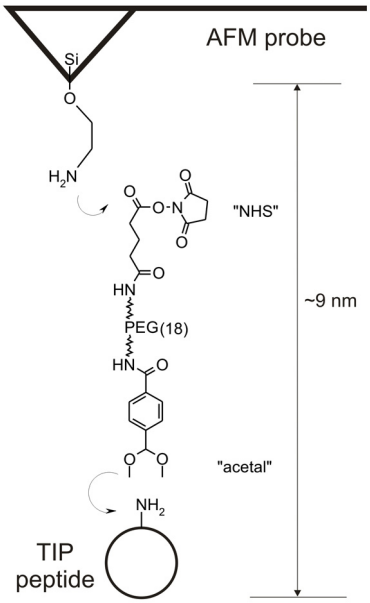

Figure 11. Functionalization scheme used in this thesis. Silicone nitride probe was modified with ethanolamine to produce -NH_2 groups for coupling with the acetal-PEG-NHS crosslinker. The TIP peptide was then attached using the free amino group of its sole lysine.

Attachment of the specific ligands

Ideally, the heterobifunctional crosslinker already carries the ligand. However this is not the case, when biopolymers (e.g. proteins, nucleic acids) are used as ligands, due to the risk of their unfolding and degradation. There are different ways to attach the ligands to the free end of the probe-linked PEG. When attaching proteins, the chemistry is largely dependent on the type of amino acids which can react covalently with the polymers. Generally these reactions are directed toward lysine and cysteine. Lysine contains a terminal amine, which can be attached to polymers conjugated with reactive esters. Cysteine, on the other hand, contains a terminal thiol, and therefore such thiol reactive groups like maleimides, vinil sulfones, and thiols (formations of disulfide) should be used (Herman *et al.,* 1994). During macromolecular

attachment it is important to know the structure of the molecule of interest, as the reaction is nonspecific in relation to where on macromolecule the attachment will occur. This is particularly important if the attachment happens to be in the vicinity or inside the binding pocket of a protein. Attachment through the polyhistidine-tag on a N- or C-terminus of the protein can help to overcome such a problem (Kienberger *et al.,* 2000).

Attachment of receptors to flat surfaces

The coupling chemistry described above is equally suited for receptor binding on flat surfaces. However, the fastest and easiest way of protein immobilization is by simple electrostatic adhesion on mica surface. Mica (muscovite) is one of the most common surfaces for AFM measurements. Other materials with silanol groups on the surface such as glass are also used. The proteins with a positive net charge can bind firmly directly to mica surface, whereas negatively charged proteins can bind only upon addition of divalent cations. It is hard however to control the strength of such electrostatic binding, meaning that some molecules of the receptor might dissociate during the experiment from the surface and bind to the ligand on the probe, resulting in an inactivated sensor. This could be overcome by intensive washing of the surface prior the experiment and use of low ionic strength buffers. Nevertheless, for most other proteins a covalent attachment, like the one for the ligand, should be preferred.

A totally different approach is required for the membranes and cells attachment, typically dependent on their nature. Biological membranes usually contain membrane proteins that will upon binding to the substrate lead to the membrane attachment. Both mammalian and bacterial cells can be trapped in pores of filters that allow their immobilization (Kasas and Ikai 1995). Upon settling, cells in suspension can also spontaneously adhere to the surface of coverslips and mica. Luckily, when dealing with adherent cell culture which grows as a monolayer, it is enough to grow them on the surface of interest. Both mica and glass coverslips showed to be perfect substrates for the cell culture, however, several cell lines tend to grow on a substrate made from plastic (polystyrene, PVC, polycarbonate, PTFE, etc.) instead. Sometimes additional pretreatment of the surface with the adhesion molecules like fibronectin or poly-L-lysine, might be useful or necessary. Most of the cell cultures require CO_2-enriched, warm environment to maintain vital growth. However, most of them are still able to withstand ambient conditions for some periods of time, enough for SMFS experiments.

2.2.2 Operation principle of the SMFS

In SMFS experiments the cantilever deflection (and not directly the force) is measured on course of the probe surface separation. The relation between the measured cantilever deflection Δx and the acting force f is given by the Hook's law:

$$f = k\Delta x \tag{1}$$

where k is the cantilever spring constant. Using very soft cantilevers (tens of pN/nm) it is possible to detect extremely low forces, down to a few piconewtons. The force resolution is mainly limited by the thermal noise of the cantilever, therefore softer cantilevers with lower spring constants show higher force sensitivity. Weak interactions (van der Waals, hydrophobic, hydrogen bonds) are usually only slighter higher than the thermal energy k_BT (where k_B is the Boltzmann constant and T is the temperature in Kelvin). However, the overall binding energy is in the range of a few to tens of k_BT, because receptor-ligand bonds are usually formed by few weak interactions. Thus they are large enough to be detected by the SMFS.

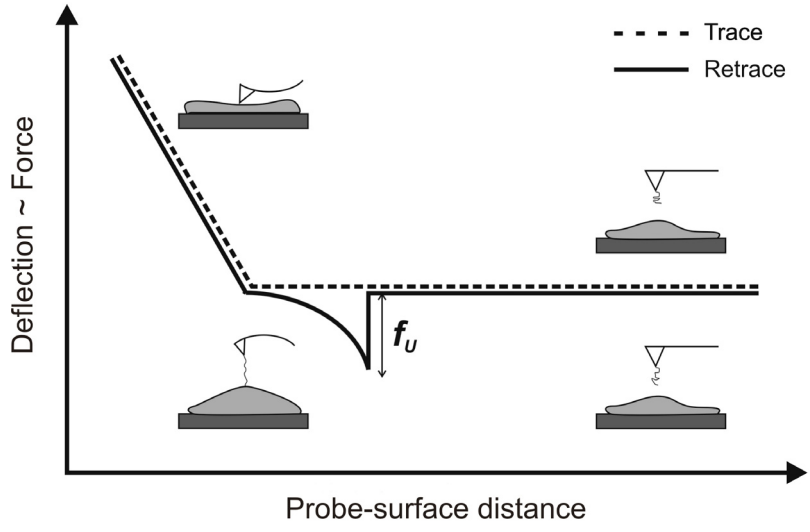

Figure 12. Schematic representation of a single-molecule recognition event between the cell and the functionalized probe.

The interaction forces in the SMFS measurements are recorded in so-called "force-distance cycles". At the beginning, the cantilever, carrying the functionalized probe, is usually about 100-1000 nm above the surface. With a constant velocity, it is then approached down towards the sample surface. From

a certain position on, the ligand and the probe contact the surface, followed by a linear rise of upward bending of the cantilever (**Fig. 12**). To avoid too high forces, the upwards bending force is usually limited to 0.5-1 nanonewtons. During the following retraction period, the bending linearly decreases and the cantilever returns into its resting position, where it looses the direct contact with the surface. If a ligand-receptor complex formation has occurred in the contact region, the further retraction of the probe causes a downwards bending of the cantilever. This additional bending event with a typical nonlinear appearance is caused by stretching of the distensible crosslinker (e.g. PEG). At the critical unbinding force, the pulling force is higher then the receptor-ligand binding, which becomes visible from a sudden rupture of the complex.

2.2.3 Dynamic SMFS

Ligand-receptor binding is generally a reversible reaction. The average lifetime of a ligand-receptor bond τ_0, is given by the kinetic off-rate k_{off}, according to:

$$\tau_0 = k_{off}^{-1} \tag{2}$$

During the SMFS measurements, a force acting on a binding complex essentially reduces its lifetime. In the thermal activation model, the lifetime $\tau(f)$ of a bond loaded with a force f is written as:

$$\tau(f) = \tau_{osc} \exp\left(\frac{E_b - lf}{kT}\right) \text{ (Bell 1978)} \tag{3}$$

where $\boldsymbol{\tau_{osc}}$ is the inverse of the natural oscillation frequency, E_b is the energy barrier for dissociation, and l is the effective length of the bond. Consequently, the lifetime $\tau(f)$ under force f compares to the lifetime at zero force τ_0, according to:

$$\tau(f) = \tau_0 \exp\left(\frac{-lf}{kT}\right) \text{ (Hinterdorfer } \textit{et al.,} \text{ 1996)} \tag{4}$$

Theoretical studies have shown that during force-distance cycles the unbinding force of specific and reversible ligand-receptor binding is dependent on the rate of the increasing force (Grubmüller *et al.,* 1996; Evans and Ritchie 1997; Izrailev *et al.,* 1997). In experiments, the unbinding forces were found to depend on both the pulling velocity and the cantilever spring constant (Lee *et*

al., 1994). Further theoretical studies revealed the logarithmic dependence of the unbinding force on the loading rate (Merkel *et al.,* 1999; Strunz *et al.,* 1999; Baumgartner *et al.,* 2000; Kienberger *et al.,* 2000). Force acting on a binding complex reduces the lifetime of the bond due to its input of energy, therefore enhancing the probability of ligand bond to dissociate. In unbinding force distribution, both force f and width of the force distribution σ_U clearly increase with increasing loading rate (Kienberger *et al.,* 2000).

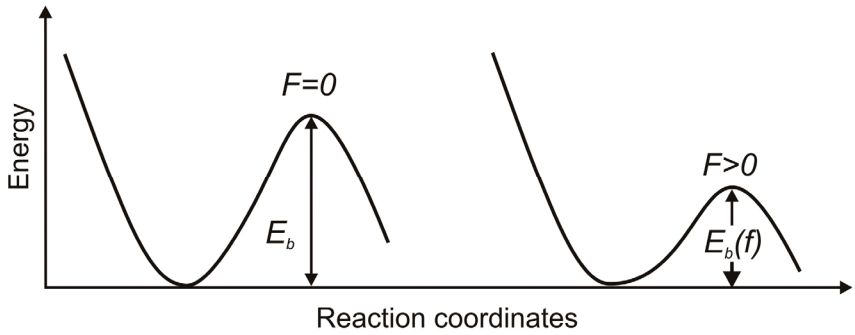

Figure 13. Schematic representation of the energetic barrier without external force (left), and under external force (right).

At slower loading rates the system adjusts closer to equilibrium which leads to smaller values of both the force f and variation of σ_U (**Fig. 14**). On a half-logarithmic scale, the unbinding force rises linear with the loading rate, which is characteristic for a single energy barrier in the thermally activated regime (Merkel *et al.,* 1999).

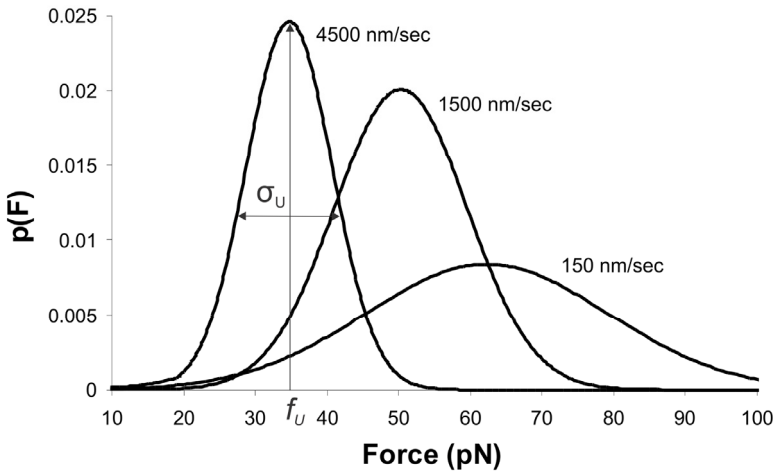

Figure 14. Unbinding force distributions between the TIP peptide and H441 cells under various pulling velocities. *p(F)* corresponds to the number of events.

Rupturing molecular bonds in SMFS experiments represent a non-equilibrium process. However, recent advances in statistical mechanics, like Jarzynski equality (Jarzynski 1997) and fluctuation theorem (Evans *et al.,* 1993) proclaim that in microscopic systems the equilibrium parameters like a free energy differences can be measured from the ensemble of non-equilibrium measurements. However, this "violation" of the second law of thermodynamics is valid only for microscopic systems and within small periods of time (Wang *et al.,* 2002; Carberry *et al.,* 2004). SMFS experiments therefore allow for estimation of equilibrium kinetic rates (like dissociation constants, K_D), and energy barrier of dissociation of the binding molecules. Estimation of the on-rate constant, k_{on} for association of a ligand with its receptor requires data of the interaction time needed for half-maximal probability of binding $t_{0.5}$. It can be experimentally determined by measuring the dependence of the binding probability on the ligand-receptor encounter duration. Knowing the effective ligand concentration c_{eff} on the probe available for receptor interaction k_{on} is given by:

$$k_{on} = 1/t_{0.5}c_{eff} \tag{5}$$

The effective concentration c_{eff} is reciprocal to the effective volume V_{eff} available for interaction, yielding:

$$c_{eff} = 1/N_A V_{eff} \tag{6}$$

where N_A is the Avogadro constant. Estimation of the off-rate constant through the lifetime of a ligand-receptor bond is described previously. The above parameters yield the equilibrium dissociation constant $K_D=k_{off}/k_{on}$ comparable to the other methods (Hinterdorfer 2002; **Publication VI**).

2.3 Molecular docking

Molecular docking is a computer-based technique that attempt to predict how molecules of known structure will interact. The knowledge of the preferred orientation then may be used to predict the strength of association or the binding affinity between two molecules. The binding geometries are often called binding modes or poses. The term "docking" is mostly related to noncovalent interactions between ligand and receptor molecules. The interactions between different molecules could be studied including a protein-ligand docking, protein-protein docking, protein-DNA docking, etc. The largest niche in the life science where molecular docking is used extensively is drug

design. The major advantage of molecular docking that makes it so desirable to use, is that it allows quickly screen large databases of potential drugs which would otherwise require tedious work in the laboratory using traditional drug discovery procedures.

Protein-ligand docking has found another important application in biomolecular science. When determining the structure of protein-ligand complex in X-ray crystallography, the positions of the protein's atoms can be determined relatively straightforwardly (by analogy with homologous proteins), the electron density of the ligand however, turns out to be often too ambiguous to assign the atomic position of its binding mode. Molecular docking may be used to identify the most favorable conformation of the ligand when bound to the protein molecule, which may then be tested with the experimental electron density map. Similarly, the binding of substrates, products and transition states may be predicted computationally, allowing study of enzyme mechanisms and bound states that are impossible to study experimentally.

2.3.1 The principle of docking

All docking experiments start with the structure of a ligand and a receptor. Experimental structures (X-ray, NMR) are always preferable. However, most X-ray structures include bound molecules of water and ions along with the ligand atoms. All of them have to be deleted except for those that have three or more polar interactions with the protein atoms and have been implicated in the mechanism of the protein function.

As in a protein folding, there are two primary concerns to consider in docking: the **search algorithm** and the **scoring function**. The first one explores the space of all possible ligand binding modes and conformations in search of a minimal energy structure. The second one evaluates the quality of the particular complex.

Search algorithms

The ideal docking method would allow both ligand and receptor to explore their conformational degrees of freedom. Perhaps the most "natural" way to do that is via a molecular dynamic simulation of the ligand-receptor complex. However, such calculations are computationally very demanding and are not capable in exploring the range of binding modes very well, except for small and mobile ligands. For many binding systems, the energy barriers that separate one binding pose from another are often to large to overcome.

a) Multiconformer docking algorithms

Here small molecules docked based on shape complementarities using multiconformer libraries to consider ligand flexibility. In matching algorithms pharmacophores of both ligand and receptor are generated to guide the docking. The distance matrices of the ligand and receptor pharmacophores are then examined for a match. If there is a match, rotational and translational vectors are calculated and position the ligand in the same frame of reference as the protein (Moitessier *et al.,* 2008).

b) Incremental constructions

In these search algorithms the ligand is initially split into a set of fragments and then builds up on-the-fly in the active site of the receptor. The first fragment called anchor is rigidly docked to the binding site using various algorithms.

c) Stochastic methods

There are various methods to search conformational space stochastically with the most common methods being **genetic algorithm** and **Monte Carlo** search. Genetic algorithm is based on Darwin's theory of evolution. The pose of the ligand represent the chromosome, in which the genes code ligand's torsion angles, as well as rotation and translation in space. The poses then evolve through transmission of the genetic information. The 'new generation' could be selected by the survival of the fittest ones, where the two lowest scoring conformations are passed to the next generation. Modifications of the genetic algorithm (e.g. Lamarckian genetic algorithm in AutoDock) have been found to efficiently explore the conformational space of the ligands. In the Monte Carlo the pose of the ligand is sequentially modified through bond rotation and translation or one or more parameters at a time and the new conformation is then evaluated. If a pose is lower in energy it is kept. If the new pose has higher energy, it could be rejected or accepted if fulfilled the Metropolis criterion (Metropolis *et al.,* 1953; Moitessier *et al.,* 2008; Yuriev *et al.,* 2010).

Utilization of more then one search algorithm in conjunction with refinement of the poses was shown to obtain higher accuracy. Any additional information regarding the ligand-receptor complex (e.g. site-directed mutagenesis study) may reduce the number of the false positives and false negatives therefore improving average performance.

Scoring functions

The measure of interaction between two molecules is usually expressed quantitatively by an energy value which is used to predict the strength of the non-covalent interaction (also referred as binding affinity). Such an attempt to approximate the standard chemical potentials of the system by mathematical

methods is known as scoring functions (SFs). SFs are a critical part of the molecular docking. The two main characteristics of the SFs are selectivity and efficiency. Selectivity enables the function to distinguish between correctly and incorrectly docked structures and efficiency enables the docking program to run in a reasonable amount of time. The simplest SFs perform rapid screening using simple geometric or steric criteria, allowing large number of ligands to be docked to a given target. The middle one are enthalpic SFs, which account for the potential energy of interaction by using pairwise-atomic Lennard-Jones potentials, 12-10 hydrogen bonding terms, and Coulombic electrostatics. These resemble the force fields commonly used in molecular mechanics and molecular dynamics programs and require moderate computational resources.

Though various types of the SFs exist nowadays, they are usually classified into three different groups: empirical, force field-based, and knowledge-based.

a) Empirical scoring functions

These SFs are suitable for a rapid ligand scoring. Initially, a number of structural descriptors, which represent the physical principles of a ligand-receptor complex formation, are selected. Then, weights are derived for each of the descriptors by regression methods using standard statistical methods (Krumrine *et al.,* 2003). Each empirical scoring function differs by the number and nature of the terms used to make up its equation. Some include an explicit directional hydrogen bond energy term. Many empirical SFs take into account the hydrophobic effect in the binding. Among the most commonly used empirical SFs is ChemScore, which has been implemented in various docking programs (e.g. Glide, GOLD, FRED).

b) Force fields or first principle methods

Force field (FF) methods use the sums of terms like bond stretching, angle bending, torsion angles, van der Waals and electrostatic interactions, to approximate the energy of a molecule complex. FFs are commonly used in molecular dynamics simulations and therefore suitable for describing the conformational change of the receptor. The FF parameters are usually derived from quantum mechanical calculations and from suitable experimental data. However, various docking programs utilize different FF parameters. Comparing to empirical SFs, a smaller number of SFs were developed from the FFs. Usually FF terms are combined with the empirical SFs, although the scaling factors to the nonbonded terms are usually applied for accurate prediction of the binding affinity in a protein-ligand complexes.

c) Knowledge-based scoring functions

The method is based upon analyzing the frequency of a particular type of a receptor's and a ligand's atom to be in a contact in a structural database of protein-ligand complexes. Higher frequencies which indicate stronger binding, is then converted into energy utilizing Boltzmann-like relationship. This approach is related to a classical statistical physical method, which uses potentials of mean force to account for all the physical forces.

The most complete SFs are those which include not only the enthalpic terms, but also entropic terms, and which estimate free energies of binding. Examples of programs that use this type of scoring function are LUDI (Böhm 1992) and AutoDock (Goodsell *et al.,* 1996). These free energies functions are often derived empirically using linear regression analysis, and require a careful calibration using a large set of structures or protein-inhibitor complexes of known binding affinity. However, they have shown better prediction of experimental binding constants than purely enthalpic force fields. The usual pitfalls of all scoring functions are their simplification and biased towards the proteins and the docking programs used to calibrate them. To overcome this, more than one scoring function can be employed with docking programs.

As an example, binding evaluation used in **AutoDock Vina** (Trott and Olson 2009) and **Glide** (Schrödinger, LLC, New York, NY) are presented here. The general functional form of the conformation-dependant part of the **AutoDock Vina** scoring function is designed to work is

$$c = \sum_{i<j} f_{t_i t_j}\left(r_{ij}\right) \tag{7}$$

where the summation is over all the pairs of atoms that can move relative to each other, normally excluding 1-4 interactions. Here, each atom i is assigned a type t_i, and a symmetric set of interaction functions $f_{t_i t_j}$ of the interatomic distance r_{ij} should be defined. This value can be seen as a sum of intermolecular and intramolecular contributions:

$$c = c_{\text{inter}} + c_{\text{intra}} \tag{8}$$

The optimization algorithm, attempts to find the global minimum of c and other low-scoring conformations, which it then ranks (Trott and Olson 2009).

Unlike the other methods, **Glide** approximates a complete systematic search of the conformational and positional space of the docked ligand. In this search, an initial rough positioning and scoring phase that dramatically narrows the search space is followed by torsionally flexible energy optimization on an OPLS-AA nonbonded potentional grid for a few hundred surviving candidate poses. The very best candidates are further refined via a Monte Carlo sampling

of pose conformation. Selection of the best docked pose uses a model energy function that combines empirical and FF-based terms. Finally the scoring is then carried out on the energy-minimized poses (*Glide 5.5 user manual, Shrödinger press*).

2.3.2 Structure flexibility in docking

Rigid versus flexible docking

Current docking methods follow the assumption that protein structures are rigid entities and that it is the ligand that changes its 3D structure to find the best spatial and energetic fit to the proteins' binding sites. This assumption follows the "lock-and-key" binding model proposed by Hermann Emil Fischer in 1890. As it was shown later, this model is not generally valid. The induced-fit model proposed by Daniel E. Koshland, Jr. in 1958, defines both protein and ligand flexible and capable of changing their conformation upon interaction forming a minimum energy complex. This model has been shown to be more realistic. Unfortunately, full scale modeling of flexible receptors during the binding process is still beyond the present computational capability. Modeling the full flexibility requires more than 1000 degrees of freedom, even for a small size protein. The compromise solution is to use a rigid receptor backbone while allowing for flexibility in the side chains near the ligand binding site.

Partial protein flexibility

The first attempt used in modeling partial protein flexibility was the soft-docking method first described by Jiang and Kim (Jiang and Kim 1991) and later improved by others (Walls and Sternberg 1992; Sandak *et al.,* 1995; Vakser 1995; Gschwend *et al.,* 1996). The principle of this method is based on decreasing the van der Waals repulsion energy term between the atoms in the binding site and those in the ligand. This method could result in solutions with physically impossible atom collisions. Nevertheless, due to the mobility available to the protein atoms in the binding site, it is possible that there is low energy rearrangement that would eliminate collisions while maintaining the conformation of the ligand returned during its conformational search. This method has the advantage of being computationally efficient as it still describes the protein using fixed coordinates and it is easy to implement since it does not require changes to the scoring function besides changing van der Waals parameters.

Full protein flexibility

The ideal way to simulate ligand docking to a protein is by using molecular dynamics (MD). This has the advantage that not only it takes into

account all the degrees of freedom available to the protein but also enables an explicit modeling of the solvent. Furthermore, accurate energy calculations can also be carried out using the free energy perturbation method.

An alternative approach to model full protein flexibility is to generate an ensemble of rigid protein conformations that together represent the conformational diversity available to the protein. Docking to an ensemble of structures generated using MD was first reported by Pang and Kozikowski (Pang and Kozikowski 1994).

Unfortunately, modeling proteins using MD is computationally expensive, and the computational power necessary to simulate the full process of diffusion and ligand binding without any approximations will be out of our reach for many years to come. However, combination of molecular docking with the following MD equilibration appears to be a good compromise utilizing the advantages of both. During the rigid docking, potential "hot spots" are being localized on the protein surface. During the following MD run the predicted binding poses are then allowed to evolve in time, marking out only the stable ones. The example of usage of such a method is presented in the current thesis **(publication III)**.

2.3.3 Limitations of molecular docking

There are two major reasons responsible for failures in molecular docking: (i) inaccuracies in the energy models used to score potential ligand/receptor complexes, and (ii) inability of used method to account for conformational changes that occur during the binding process not only for the ligand, but also for the receptor. Simulation of a flexible ligand to a rigid biological receptor does not reflect the actual physical process of binding and limits or in some cases even prevents the correct identification of potential drug candidates.

Most docking algorithms are able to generate a large number of possible structures, and so they also require a means to score each structure to identify those of desired usefulness. The "docking problem" is thus concerned with the generation and evaluation of plausible structures of intermolecular complexes (Blaney and Dixon 1994).

2.4 Molecular dynamics simulations

2.4.1 Introduction

Molecular dynamics (MD) simulations represents a principal method among the tools used in the theoretical study of biological molecules. This method unites theoretical routines and computational techniques to model or to mimic the behavior of the molecules, and is a specialized discipline of the molecular modeling based on statistical mechanics. MD simulations generate information at the microscopic level, including atomic positions and their potentials. The conversion of this microscopic information to macroscopic observables such as pressure, energy, heat capacities, etc., requires statistical mechanics. In a regular laboratory experiment using a macroscopic sample, enormous numbers of conformations are usually sampled. In the statistical mechanics, averages corresponding to experimental observables are defined in terms of ensemble averages. Therefore, the goal of a MD simulation is to run long enough to generate representative conformations that will be arbitrarily close to every possible microstate. Thus, experimentally relevant information concerning structural, dynamic and thermodynamic properties may then be calculated using a feasible amount of computer resources.

Apart from MD, the quantum mechanical methods are also widely used in the "*in silico* biology" (Gogonea *et al.,* 2001). The quantum mechanical methods are based on the solution of the Schrödinger equation and allow for explicit representation of the electrons in calculations. That makes possible to derive properties that depend upon electronic distribution, and therefore investigate chemical reactions in which bonds are broken and formed. Despite of their advantage, quantum mechanical methods are extremely demanding on the computational power, and therefore are not yet feasible for larger systems including large biomolecular systems.

Molecular mechanics (also referred to as the force-field or potential energy methods) comparing to the quantum mechanical methods uses Newtonian mechanics to model molecular systems. Electronic motions are ignored and energy of the system is calculated as a function of the nuclear positions only. In the molecular mechanics a molecule is considered as a collection of masses centered at the nuclei (atoms) connected by springs (bonds), which in response to inter- and intramolecular forces can stretch, bend and rotate. The basic principle of the molecular mechanics is that collective physical forces can be used to describe molecular geometries and energies. This simple description of a molecular system as a mechanical body generally works well for describing molecular structures and processes, with the exception of bond-breaking events (Schlick 2010).

The two most common simulation techniques used in the molecular modeling are the MD simulations and the Monte Carlo method. Since the MD simulations were used in this thesis, it therefore will be described in a more detail here.

2.4.2 History

The MD simulation was first introduced by Alder and Wainwright in the late 1950's (Alder and Wainwright 1957, 1959) to study the interactions of hard spheres. Many important insights concerning the behavior of simple liquids emerged from their studies. The first molecular dynamics simulation of a realistic system was done by Rahman and Stillinger in their simulation of liquid water in 1971 (Rahman and Stilling.Fh 1971). The first protein simulations appeared in 1977 with the simulation of the bovine pancreatic trypsin inhibitor (McCammon *et al.,* 1977). Nowadays, the MD simulations of solvated proteins, membrane proteins in a lipid bilayer, and protein-DNA complexes are being published regularly. The combinations of the quantum mechanical and classical simulations to study enzymatic reactions have been reported (Aqvist and Warshel 1993; Zhang 2006). MD simulation techniques are widely used in experimental procedures such as X-ray crystallography and NMR structure determination.

2.4.3 Principle

The MD simulation methods are based on Newton's second law or the equation of motion, $F_i=m_i a_i$ for each atom i in a system composed by N atoms. Here, m_i is the atom mass, $a_i=d^2r_i/dt^2$ its acceleration, and F_i the force acting upon it, due to the interaction with the other atoms (Schlick 2010). Knowing the force that acts on each atom, it is possible to determine the acceleration of each atom in the system. Integration of the equations of motion then yields a trajectory that describes the positions, velocities and accelerations of the particles as they vary with time. The method is deterministic; once the positions and velocities of each atom are known, the state of the system can be predicted at any time in the future or the past. The advantage of this method is that it enables to follow and understand structure and dynamics on atomic scales.

The force acting on each particle will change whenever the particle changes its position, or whenever any of the other particles with which it interacts change their positions. Under the influence of the continuous potential the motions of all the particles are coupled together, giving rise to a many-body problem that cannot be solved analytically. Under such circumstances the

equations of motion are integrated using a finite difference method. This method is used to generate molecular dynamics trajectories with continuous potential models. The integration is broken down into many small stages, each separated in time by a fixed time Δt (typically between 1-10 femtoseconds).

The total force acting on each particle in the configuration at a time t is calculated as the vector sum of its interactions with other particles, which are then combined with the positions and velocities at a time t to calculate the positions and velocities at a time $t+\Delta t$. The force is assumed to be constant during the time step. The atoms are then moved to a new positions and an updated set of forces is computed (Leach 2001).

Various numerical methods are used to integrate Newton's equation of motion. Among them are: the Verlet algorithm (Verlet 1967), the leap-frog algorithm (Hockney 1970), the velocity Verlet (Swope *et al.,* 1982), Beeman's algorithm (Beeman 1976), the predictor-corrector method (Gear 1971). The MD program used in this thesis (YASARA Structure ver. 11.6.16, Krieger *et al.,* 2002) utilizes the leap-frog method. In the leap-frog algorithm, the velocities are first calculated at time $t+\Delta t/2$, and then are used to calculate the positions x at time $t+\Delta t$:

$$x(t+\Delta t) = x(t) + V\Delta t\left(t + \frac{\Delta t}{2}\right) \tag{9}$$

where V is velocity. Therefore, the velocities leap over the positions, and then the positions leap over the velocities. The advantage of this algorithm is that the velocities are explicitly calculated, however, the disadvantage is that they are not calculated at the same time as the positions. The velocities at time t can be approximated by the relationship:

$$V(t) = \frac{1}{2}\left[V\left(t + \frac{\Delta t}{2}\right) + V\left(t - \frac{\Delta t}{2}\right)\right] \text{(Leach 2001)} \tag{10}$$

2.4.4 Force fields

All classical simulations methods to calculate interactions and evaluate the potential energy of the system as a function of point-like atomic coordinates rely mainly on empirical approximations called force fields (FF). The FFs consists of both: (i) the set of equations used to calculate the potential energy and forces from particle coordinates, and (ii) a collection of parameters used in the equations. For most of the purposes these approximations work well, but they cannot reproduce quantum effects like bond formation or breaking.

Potential functions in the force fields are usually subdivided in two classes: bonded interactions and nonbonded interactions. Bonded interactions include covalent bond-stretching, angle-bending, torsion potentials when rotating around bonds, and out-of-plane "improper torsion" potentials. The nonbonded interactions consist of Lennard-Jones repulsion and dispersion and electrostatic (Coulombic) potential (**Fig. 15**). The accuracy of a FF depends strongly on its parameters (e.g. Van der Waals radii, atomic charges). In this thesis a novel self-parameterizing force field was used (Yamber3, Krieger *et al.,* 2009). The initial parameters of such a force field change randomly during the energy minimization of the model, and then are either accepted if the model improved, or rejected if did not (Krieger *et al.,* 2003).

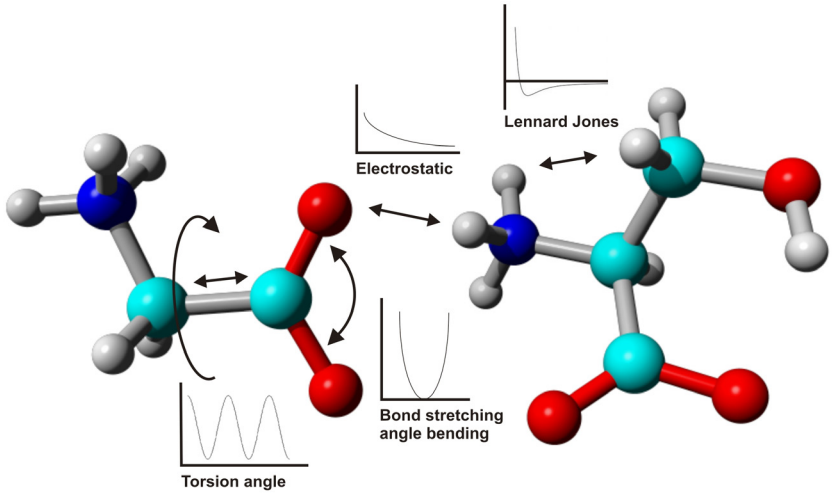

Figure 15. Schematic representation of the intra- and interatomic potentials.

Typical biomolecular simulations apply periodic boundary conditions to avoid surface artifacts, so that a solvent molecule that exits to the right of a simulation box reappears on the left. The box however, should be large enough that the molecules will not interact significantly with their periodic copies. This is intimately related to the non-bonded interactions, which ideally should be summed over all neighbors in the resulting infinite periodic system. Simple cut-offs can be applied for Lennard-Jones interactions that decay very rapidly, but for Coulomb interactions a sudden cut-off can lead to large errors. One alternative is to "switch off" the interaction before the cut-off, but a better option is to use particle-mesh Ewald (PME) summation (Darden *et al.,* 1999) to calculate the infinite electrostatic interactions by splitting the summation into short- and long-range parts. For PME summation, the cut-off only determines the balance between the two parts, and the long-range part is treated by

assigning charges to a grid that is solved in a reciprocal space through Fourier transforms.

Cut-offs and rounding errors can lead to drifts in energy, which will cause the system to heat up during the simulation. To control this, the system is normally coupled to a thermostat that scales velocities during the integration to maintain preset temperature. Similarly, the total pressure in the system can be adjusted through scaling the simulation box size, either isotropically or separately in x-y-z dimensions.

Internal motions	Timescale (seconds)
Light atom bond stretching	10^{-14}
Double bond stretching	2×10^{-14}
Light atom angle bending	2×10^{-14}
Heavy atom bond stretching	3×10^{-14}
Heavy atom angle bending	5×10^{-14}
Global DNA twisting	10^{-12}
Surface-sidechain rotation (protein)	10^{-11}–10^{-10}
Global DNA bending	10^{-10}–10^{-7}
Interior sidechain rotation (protein)	10^{-4}–1
Protein folding	10^{-5}–10

Table 2. Timescales in biomolecules (adopted from Schlick 2010).

The single most demanding part of simulations is the computation of non-bonded interactions, since millions of pairs have to be evaluated for each time step. Extending the time step is thus an important way to improve simulation performance, but unfortunately errors are introduced in bond vibrations already at one femtosecond. However, in most simulations the bond vibrations are not of interest by itself and can be removed entirely by introducing bond constraint algorithms (e.g. SHAKE, Ryckaert *et al.,* 1977; LINCS, Hess *et al.,* 1997; SETTLE, Miyamoto and Kollman 1992).

2.4.5 Molecular dynamics limitations

MD simulations is a very powerful technique but has of course limitations which mainly originate in approximations been used. Since all interactions are treated purely by classical mechanics, neither chemical reaction, meaning bond breaking or formation or electron transfer, nor events faster then integration time step can be followed. The size of the system that can be mimicked by MD simulations is of many orders of magnitude smaller then any

real one. Among the most prominent limitations of the MD simulation techniques are the following:

- **Usage of classical forces**
  It is well known that systems at atomistic levels obey quantum laws rather then classical laws, and therefore Schrödinger's equation should be used. However, its application to the large biological models is insufficient up to now.
- **Realism of forces**
  Since the forces are usually obtained as the gradient of a potential energy function depending on position of the particles, the realism of the simulation therefore depends on the ability of the chosen potential to reproduce the behavior of the object under simulation conditions. Thus, proper potentials should be selected.
- **Time**
  The typical MD simulations are performed on systems containing thousands to millions of atoms with the simulation time ranging from a few picoseconds to hundreds of nanoseconds. To be "safe", a simulation should be run longer then the relaxation time of the quantities of interest (**Table 2**). However, different properties have different relaxation times and that should be taking into account before initializing the simulation run.
- **Size**
  A limited system size can also constitute a problem. In this case one has to compare the size of the MD cell with the correlation lengths of the spatial correlation functions of interest. This problem is partially solved by using simulation cell with periodic boundaries, thus mimicking the infinity of the cell. Special attention however should be paid to the truncation of the long range potentials, which when neglected could lead to the interaction of the object with itself.

Chapter 3

Results and Discussion

Does the TIP peptide interact with the molecules located on the apical side of the lung epithelial cells?

Administration of the TIP peptide to the apical but not to the basolateral side of the primary rat alveolar type 2 epithelial cells was shown to significantly increase the transepithelial current (Hamacher *et al.,* 2010). Also, intratracheal but not intravenous administration of the TIP peptide leads to the efficient activation of the alveolar liquid clearance both *ex vivo* and *in vivo* (Elia *et al.,* 2003; Braun *et al.,* 2005; Hamacher *et al.,* 2010). Collectively, these results indicate polarity in the TIP peptide's action. ENaC is one of the molecules that are expressed in the apical membrane of the lung epithelial cells (Renard *et al.,* 1995; Farman *et al.,* 1997) and plays a key role in mediating the first step of active Na^+ reabsorption in maintaining lung electrolyte and water homeostasis (Garty and Palmer 1997). Several recent findings support the direct or indirect activation of the ENaC by the TIP peptide (Hamacher *et al.,* 2010; Hazemi *et al.,* 2010). However, no interaction of the TIP peptide with the lung epithelial cells was reported so far. Moreover, the inability of the TIP peptide to interact with liposomes (van der Goot *et al.,* 1999) pointed towards a peptide-protein or peptide-carbohydrate nature of the TIP peptide interaction in mediating its activity. The TIP peptide-carbohydrate interaction was later confirmed by high-resolution mass spectrometry study using the pure TIP peptide and disaccharides *N,N'*-diacetylchitobiose and cellobiose (Marquardt *et al.,* 2007). To investigate the possibility that the TIP peptide interacts with surface molecules of H441 cells, we have carried out single-molecule force spectroscopy experiments. Their goal was to discover possible specific interactions between the single TIP peptide and single molecules localized on the apical side of the H441 cells. Such specific interactions were observed with the ~10% occurrence, which is a typical value for the SMFS experiments on live cells (Puntheeranurak *et al.,* 2006; Puntheeranurak *et al.,* 2007; Wildling *et al.,* 2011). The unbinding forces were 50±13 pN at a pulling velocity of 1500 nm/sec.

The specificity of interaction was proven by adding *N,N'*-diacetylchitobiose (0.2 mg/ml final concentration), which blocked the interactions by 55 %. (down to 4.5%) The remaining binding that was present after adding the *N,N'*-diacetylchitobiose could represent the margin between the specific and unspecific binding of the TIP peptide to the cell's apical surface. Interestingly, marginal (~27%) activity of *N,N'*-diacetylchitobiose-blocked TIP peptide was observed in trypanolysis experiments (Lucas *et al.,* 1994). Another disaccharide, i.e. cellobiose, that was shown not to inhibit the TIP peptide-mediated effects (Lucas *et al.,* 1994; Hribar *et al.,* 1999) and having >20-fold

lower binding affinity to the TIP peptide than *N,N'*-diacetylchitobiose (Marquardt *et al.,* 2007), has shown no inhibitory effects in our experiments (0.5 mg/ml final concentration).

As it was predicted (Bell 1978) and proven later (Evans and Ritchie 1997) the unbinding force of the individual ligand-receptor complex increases with increasing loading rate (or pulling velocity). By performing the SMFS pulling experiment at various velocities, it was therefore possible to apply various pulling forces to the TIP peptide-surface molecules of the H441 cells. Fitting the data and using **Eq. 4** we have shown that the lifetime of the TIP peptide complex with the surface molecules was decreasing from 2.3 ms at 34 pN to 0.1 ms at 62 pN. Data fit also yielded the lifetime at zero force, τ_0=262 ms, which corresponds to a kinetic off-rate of k_{off}=3.81 s^{-1}.

The TIP peptide's amino acids T6, E8, and E11 were shown to be crucial in mediating its activities, since the mutated TIP peptide (mutTIP) having these residues mutated to alanines and the scrambled TIP peptide (scrTIP) having the same amino acids as the TIP peptide but in a random order were shown to be inactive (Lucas *et al.,* 1994; Hribar *et al.,* 1999; Elia *et al.,* 2003; Braun *et al.,* 2005; Vadász *et al.,* 2008; Hamacher *et al.,* 2010; Hazemi *et al.,* 2010; Xiong *et al.,* 2010). To assess the importance of these crucial residues in the ability of the TIP peptide to interact with the surface molecules of the H441 cells, the mutTIP as well as the scrTIP peptides were used in SMFS measurements. The marginal binding of the mutTIP to the surface of the H441 cells was observed with 2% binding probability at twice lower unbinding forces (25±4.5 pN) as compared to the native TIP peptide. Even lower binding (1.5%) was observed when the scrTIP peptide was used. These results indicate that the residues T6, E8, and E11 of the TIP peptide are of a crucial importance in the complex formation between the TIP peptide and surface molecules on the H441 cells.

Early whole-cell voltage clamp experiments with the TIP peptide have shown that in a slightly acidic environment (pH=6.0) the TIP peptide is twice more potent in generating membrane conductance in the MVEC and in the peritoneal macrophages than under physiological conditions (pH=7.3) (Hribar *et al.,* 1999). A possible interpretation of such an effect could be a stronger binding between the TIP peptide and its putative receptor(s) leading to the lowering of its dissociation constant (K_D). To verify that, we have performed SMFS measurements at pH=5.6, which have shown however lower unbinding forces (30±14 pN) between the TIP peptide and cell's surface, while unaffecting the binding probability. No plausible explanation for this effect was available until the TIP peptide's charges at pH=5.6 and pH=7.3 were calculated (http://www.scripps.edu/~cdputnam/protcalc.html), showing that at the acidic pH the TIP peptide has smaller negative charge (−0.8), than at the neutral one (−1.3). Based on that, the SMFS results could be interpreted in a way that at the lower pH the TIP peptide interacts with its receptor(s), however with a fewer

intermolecular bonds and therefore with the lower unbinding forces. The potency of the TIP peptide in generating higher membrane conductance at the acidic pH could be thus addressed not only to the properties of the TIP peptide alone, but also to the properties of its putative receptor(s) at the acidic pH.

Collectively, the SMFS results showed the ability of the TIP peptide to interact with the surface of the H441 cells. The binding had both a specific and an unspecific component, as shown upon preincubation the TIP peptide with *N,N'*-diacetylchitobiose. The mutTIP peptide and scrTIP peptide demonstrated only non-specific binding, highlighting the importance of crucial amino acids in the TIP peptide binding to its putative receptor(s). At acidic pH the TIP peptide has shown weaker interaction with the H441 cells, which could be due to its smaller negative charge.

Does the TIP peptide need to be internalized inside of the cells to trigger its effects?

The initial process of binding of the TIP peptide to the cell's surface could be in principle followed by either (i) direct activation of a receptor molecule or by (ii) passive or active crossing of the peptide through the cell membrane with subsequent intracellular activation of the TIP peptide-mediated processes. It is not clear yet which path is followed upon the TIP peptide binding. We have tried to answer this question by comparing physicochemical properties of the TIP peptide with the physicochemical properties of the known membrane penetrating peptides. Also, direct labeling of the TIP peptide with the fluorescent dye and it subsequent administration to the H441 cells was performed.

Twenty delivery peptides were analyzed, based on their hydropathy index (Kyte and Doolittle 1982) and a net charge at pH=7.4 was evaluated. These calculations showed that: (i) most of the peptides (70%) possess the positive charge, (ii) those that have negative charge (usually >–0.2) have a positive (usually >20) hydropathy index, and (iii) none of them have both negative charge and negative hydropathy index (see **Table 1**). On the contrary, the TIP peptide appears to have both a negative charge and a negative hydropathy index, showing that its physicochemical properties are different from that of the delivery peptides.

Labeling of the TIP peptide with a small fluorescent dye enables direct localization of the TIP peptide on the surface of or inside live H441 cells. A small fluorophore (~1/4 of the TIP peptide's mass) was covalently attached using the amino group of the TIP peptide's only lysine residue, as in the SMFS experiments. The ability of the labeled TIP peptide to mediate transepithelial current in a monolayer of the H441 cells was tested in the Ussing chamber,

showing that the labeled TIP peptide has the same activity as the native one (**Fig. 4**). After preincubation of the culture of the H441 cells with the fluorescently labeled TIP peptide, they were imaged using laser scanning confocal microscope. The fluorescent signal of the labeled TIP peptide was mainly localized on the surface of the cell's plasma membrane, with no signs of the internal distribution (**Fig. 3**).

Taking together, results based on the labeling of the H441 cells with the fluorescent TIP peptide and the analysis of the TIP peptide's physicochemical properties suggest that internalization of the TIP peptide is not required for its activity and is highly unlikely.

What is the nature of the interaction between the TIP peptide and its putative receptor(s)?

To understand the nature of the interaction between the TIP peptide and its putative receptor(s), we have studied TIP peptide-*N,N'*-diacetylchitobiose, TIP peptide-cellobiose, and TIP peptide-trimannose-*O*-ethyl interactions. The idea was that since the *N,N'*-diacetylchitobiose is able to abrogate the activity of the TIP peptide as well as its specific binding to the lung epithelial cells, it could therefore bind to the same region of the TIP peptide which is implicated in its interaction with putative receptor(s). Localization of that region and identification of its residues could therefore provide valuable information about the nature of the TIP peptide's interaction with its putative receptor(s). The prerequisite of such a study is the availability of the 3D structure of the TIP peptide and the corresponding oligosaccharides. Though the 3D structures of a large variety of sugars are available through the various databases, the 3D structure of the TIP peptide is still unknown. We have used two vastly different approaches to obtain the 3D structure of the TIP peptide: molecular modeling and macromolecular crystallization. The first method is purely computational, whereas the second one requires growing the TIP peptide crystals suitable for the X-ray diffraction analysis. The second method is always associated with the most reliable and trusted models and therefore was of great importance. Unfortunately, although crystals of the TIP peptide were obtained, their diffraction was not suitable for structure determination (**Fig. 5**). Therefore, we had to rely on the molecular modeling method, which is however not so precise, yet could still provide satisfying models, especially for such small objects like the TIP peptide. The TIP peptide model was built using the molecular modeling method and was further equilibrated using MD simulations. It has shown very good structural parameters having 81.9% of its residues in most favored regions (according to the Ramachandran plot) with the overall G-score value of 0.2 (Laskowski *et al.,* 1993). More importantly, the 3D structure of the TIP peptide

was in good agreement with the 3D structure of the lectin-like domain of the TNF (PDB ID: 1TNF), with the distances among the T6-T105, E8-E107 and E11-E110 α-carbon atoms below 0.2 nm. The TIP peptide model was docked with *N,N'*-diacetylchitobiose, cellobiose, and trimannose-*O*-ethyl, and the peptide-oligosaccharide complexes were further equilibrated using MD simulations. Since it was not possible to discriminate among the affinities of used oligosaccharides to the TIP peptide, during the 100 ns of the MD run, steered MD simulations (under constant accelerations) were used. Using this method, *N,N'*-diacetylchitobiose was shown to possess the highest, trimannose-*O*-ethyl the medium, and cellobiose the lowest affinity to the TIP peptide. This finding for the oligosaccharides *N,N'*-diacetylchitobiose and cellobiose is in an agreement with a reported mass spectrometry study (Marquardt *et al.,* 2007). There was no experimental study conducted on the interaction of the trimannose-*O*-ethyl with the TIP peptide so far. However, trimannose-*O*-ethyl as well as *N,N'*-diacetylchitobiose were shown to block the interaction of native TNF through its lectin-like domain with the immunosuppressive glycoprotein uromodulin (Sherblom *et al.,* 1988). There it was shown that *N,N'*-diacetylchitobiose is a three times more potent inhibitor than trimannose-*O*-ethyl, which in our case could be viewed as a better binder. Interestingly, the best binding places for all oligosaccharides were localized on the *inner* side of the TIP peptide with respect to the lectin-like domain of the TNF (see **publication III** for details). The residues that encompass that region and are involved in hydrogen bonds formation between the TIP peptide and the oligosaccharides (*N,N'*-diacetylchitobiose and trimannose-*O*-ethyl) are R4, E5, T6, P7, P14, and Y16. Crucial amino acids T6 and E8, but not E11 were involved in the hydrogen bond formations, particularly in stabilizing the transition binding state, as well as in increasing overall negative charge of the TIP peptide. Though the importance of the crucial amino acids of the TIP peptide in binding the *N,N'*-diacetylchitobiose was reported, it was also shown that they are not a prerequisite for the TIP peptide- *N,N'*-diacetylchitobiose interaction (Marquardt *et al.,* 2007). Recent results have demonstrated the importance of the bulky hydrophobic region introduced by hydrophobic side chains of the P14, W15, and Y16 residues, as an essential feature of the TIP peptide for ENaC activation (Hazemi *et al.,* 2010). Our results obtained computationally have shown that amino acids P14 and Y16 are important in TIP peptide-oligosaccharide binding by introducing the hydrogen bonding. This leads to the conclusion that the aforementioned residues play a key role not only in the mechanism of the TIP peptide inhibition, but also in its interactions with its putative receptor(s).

What is the TIP peptide's receptor on the apical surface of the lung epithelial cells?

Even though the aim of this thesis was to tackle the initial stages of the TIP peptide action, and particularly its interaction with lung epithelial cells *in vitro*, it was very tempting not to try to identify the TIP peptide's putative receptor(s). This goal could be accomplished by different ways and using various techniques. Here we have used the affinity chromatography method, where the TIP peptide by itself was used as a functional group to isolate and purify its putative receptor(s). This method was chosen in view of the results obtained using SMFS, which have confirmed a specific interaction between the TIP peptide with its putative receptor(s). However not a single but rather a group of molecules that have an affinity to the TIP peptide were isolated (**Fig. 6**). This could also explain the occurrence of the unspecific binding exhibited by the TIP peptide during the SMFS experiments. Further mass spectrometric characterization of the isolated proteins, that could potentially answer the raised question was however unsuccessful due to the too sparse amount of isolated proteins. Interestingly, the major bands of the isolated proteins had their molecular weights around 37-50 kDa, whereas the ENaC subunits are expected to be: α – 75.7 kDa, β – 72 kDa, and γ – 74.9 kDa (Canessa *et al.,* 1994). This could be the first indirect evidence of the inability of the TIP peptide to interact directly with ENaC but rather activate it through some unknown receptor.

Chapter 4

Conclusion

4.1 Conclusion

The work summarized in this thesis was done to uncover the unknown mechanisms of the TNF-derived TIP peptide action, with relevance to pulmonary edema treatment. Several questions regarding the initial steps of the TIP peptide function that were raised in this thesis were approached and answered in a systematic way. Novel single-molecule techniques were used mostly for their sensitivity and specificity and have provided valuable information about the residues involved in the interaction of the TIP peptide with its binding partners.

4.2 Future work

Further study is required to understand the mechanisms of the TIP peptide function. Among these are those that were initiated already but failed to provide valuable results due to the technical difficulties.

4.2.1 TIP peptide structure determination

Understanding the mechanisms of the TIP peptide work will require the knowledge of its 3D structure. Further optimization of the crystallization conditions will allow obtaining the crystals of the TIP peptide suitable for the X-ray diffraction analysis. Co-crystallization of the TIP peptide with the *N,N'*-diacetylchitobiose may potentially stabilize the TIP peptide, allowing to reach this goal. Also, due to its small size and stability, the TIP peptide is a perfect object for NMR spectroscopy. The advantage of this method is that the 3D structure of the TIP peptide in solution rather then in a crystal can be determined.

4.2.2 Putative receptor(s) identification

Unfortunately, the TIP peptide receptor(s) was not identified. Large scale cell production will allow to substantially increase the quantity of the isolated proteins, whereas only apical cell membranes isolation should increase the sensitivity of the used method. Both these factors should allow finding the potential TIP peptide receptor(s).

.

Chapter 5

References

Abi-Antoun, T., Shi, S., Tolino, L. A., Kleyman, T. R., and Carattino, M. D. (**2011**) "Second transmembrane domain modulates epithelial sodium channel gating in response to shear stress". *American Journal of Physiology Renal Physiology **300***, F1089-1095.

Alder, B. J., and Wainwright, T. E. (**1957**) "Phase transition for a hard sphere system". *Journal of Chemical Physics **27***, 1208-1209.

Alder, B. J., and Wainwright, T. E. (**1959**) "Studies in molecular dynamics .1. General method". *Journal of Chemical Physics **31***, 459-466.

Allen, F. H., Kennard, O., Watson, D. G., Brammer, L., Orpen, A. G., and Taylor, R. (**1987**) "Tables of bond lengths determined by X-ray and neutron diffraction. Part 1. Bond lengths in organic compounds". *Journal of the Chemical Society, Perkin Transactions **2***, S1-S19.

Allenspach, R., Salemink, H., Bischof, A., and Weibel, E. (**1987**) "Tunneling experiments involving magnetic tip and magnetic sample". *Zeitschrift für Physik B Condensed Matter **67***, 125-128.

Alwi, I. (**2010**) "Diagnosis and management of cardiogenic pulmonary edema". *Acta Medica Indonesiana **42***, 176-184.

Ananthraman, A., Israel, R. H., and Magnussen, C. R. (**1983**) "Pleural-pulmonary aspects of *Listeria monocytogenes* infection". *Respiration **44***, 153-157.

Antos, J. M., Popp, M. W. L., Ernst, R., Chew, G. L., Spooner, E., and Ploegh, H. L. (**2009**) "A straight path to circular proteins". *Journal of Biological Chemistry **284***, 16028-16036.

Aqvist, J., and Warshel, A. (**1993**) "Simulation of enzyme-reactions using valence-bond force-fields and other hybrid quantum-classical approaches". *Chemical Reviews **93***, 2523-2544.

Baez, A. V. (**1956**) "Is resolving power independent of wavelength possible? An experiment with a sonic "macroscope"". *Journal of the Optical Society of America **46***, 901-901.

Baldwin, R. L. (**1996**) "Why is protein folding so fast?". *Proceedings of the National Academy of Sciences of the United States of America **93***, 2627-2628.

Baumgartner, W., Hinterdorfer, P., Ness, W., Raab, A., Vestweber, D., Schindler, H., and Drenckhahn, D. (**2000**) "Cadherin interaction probed by atomic force microscopy". *Proceedings of the National Academy of Sciences of the United States of America **97***, 4005-4010.

Becker, R. S., Golovchenko, J. A., and Swartzentruber, B. S. (**1987**) "Atomic-scale surface modifications using a tunnelling microscope". *Nature **325***, 419-421.

Beeman, D. (**1976**) "Some multistep methods for use in molecular-dynamics calculations". *Journal of Computational Physics **20***, 130-139.

Bell, G. I. (**1978**) "Models for the specific adhesion of cells to cells". *Science **200***, 618-627.

Binnig, G., Quate, C. F., and Gerber, C. (**1986**) "Atomic force microscope". *Physical Review Letters **56***, 930-933.

Binnig, G., Rohrer, H., Gerber, C., and Weibel, E. (**1982**) "Surface studies by scanning tunneling microscopy". *Physical Review Letters **49***, 57.

Birukova, A. A., Birukov, K. G., Adyshev, D., Usatyuk, P., Natarajan, V., Garcia, J. G., and Verin, A. D. (**2005**) "Involvement of microtubules and Rho pathway in TGF-β1-induced lung vascular barrier dysfunction". *Journal of Cellular Physiology **204***, 934-947.

Blaney, J. M., and Dixon, J. S. (**1994**) "Distance geometry in molecular modeling". *Reviews in Computational Chemistry V **5***, 299-335.

Böhm, H.-J. (**1992**) "The computer program LUDI: a new method for the de novo design of enzyme inhibitors". *Journal of Computer-Aided Molecular Design **6***, 61-78.

Braun, C., Hamacher, J., Morel, D. R., Wendel, A., and Lucas, R. (**2005**) "Dichotomal role of TNF in experimental pulmonary edema reabsorption". *Journal of Immunology **175***, 3402-3408.

Butt, H. J., Wolff, E. K., Gould, S. A., Dixon Northern, B., Peterson, C. M., and Hansma, P. K. (**1990**) "Imaging cells with the atomic force microscope". *Journal of Structural Biology **105***, 54-61.

Canessa, C. M., Schild, L., Buell, G., Thorens, B., Gautschi, I., Horisberger, J. D., and Rossier, B. C. (**1994**) "Amiloride-sensitive epithelial Na^+ channel is made of three homologous subunits". *Nature **367***, 463-467.

Cappella, B., and Dietler, G. (**1999**) "Force-distance curves by atomic force microscopy". *Surface Science Reports **34***, 1-+.

Carberry, D. M., Reid, J. C., Wang, G. M., Sevick, E. M., Searles, D. J., and Evans, D. J. (**2004**) "Fluctuations and irreversibility: an experimental demonstration of a second-law-like theorem using a colloidal particle held in an optical trap". *Physical Review Letters **92***, 1-4.

Carswell, E. A., Old, L. J., Kassel, R. L., Green, S., Fiore, N., and Williamson, B. (**1975**) "An endotoxin-induced serum factor that causes necrosis of tumors". *Proceedings of the National Academy of Sciences of the United States of America **72***, 3666-3670.

Chowdhury, P. B., and Luckham, P. F. (**1998**) "Probing recognition process between an antibody and an antigen using atomic force microscopy". *Colloids and Surfaces A: Physicochemical and Engineering Aspects **143***, 53-57.

Chtcheglova, L. A., Waschke, J., Wildling, L., Drenckhahn, D., and Hinterdorfer, P. (**2007**) "Nano-scale dynamic recognition imaging on vascular endothelial cells". *Biophysical Journal **93***, L11-L13.

Colchero, J., Luna, M., and Baro, A. M. (**1996**) "Lock-in technique for measuring friction on a nanometer scale". *Applied Physics Letters **68***, 2896-2898.

Craik, D. J. (**2006**) "Seamless proteins tie up their loose ends". *Science **311***, 1563-1564.

Craik, D. J., Daly, N. L., Mulvenna, J., Plan, M. R., and Trabi, M. (**2004**) "Discovery, structure and biological activities of the cyclotides". *Current Protein & Peptide Science **5***, 297-315.

Dagata, J. A., Schneir, J., Harary, H. H., Evans, C. J., Postek, M. T., and Bennett, J. (**1990**) "Modification of hydrogen-passivated silicon by a scanning tunneling microscope operating in air". *Applied Physics Letters **56***, 2001-2003.

Dai, H., Hafner, J. H., Rinzler, A. G., Colbert, D. T., and Smalley, R. E. (**1996**) "Nanotubes as nanoprobes in scanning probe microscopy". *Nature **384***, 147-150.

Darden, T., Perera, L., Li, L., and Pedersen, L. (**1999**) "New tricks for modelers from the crystallography toolkit: the particle mesh Ewald algorithm and its use in nucleic acid simulations". *Structure **7***, R55-R60.

Daulouede, S., Bouteille, B., Moynet, D., De Baetselier, P., Courtois, P., Lemesre, J. L., Buguet, A., Cespuglio, R., and Vincendeau, P. (**2001**) "Human macrophage tumor necrosis factor (TNF)-α production induced by *Trypanosoma brucei gambiense* and the role of TNF-α in parasite control". *Journal of Infectious Diseases **183***, 988-991.

Desjobert, C., de Soultrait, V. R., Faure, A., Parissi, V., Litvak, S., Tarrago-Litvak, L., and Fournier, M. (**2004**) "Identification by phage display selection of a short peptide able to inhibit only the strand transfer reaction catalyzed by human immunodeficiency virus type 1 integrase". *Biochemistry **43***, 13097-13105.

Diakov, A., Nesterov, V., Mokrushina, M., Rauh, R., and Korbmacher, C. (**2010**) "Protein kinase B alpha (PKBα) stimulates the epithelial sodium channel (ENaC) heterologously expressed in *Xenopus laevis* oocytes by two distinct mechanisms". *Cellular Physiology and Biochemistry **26***, 913-924.

Eastman, T., and Zhu, D. M. (**1996**) "Adhesion forces between surface-modified AFM tips and a mica surface". *Langmuir **12***, 2859-2862.

Ebner, A., Kienberger, F., Stroh, C. M., Gruber, H. J., and Hinterdorfer, P. (**2004**) "Monitoring of glass derivatization with pulsed force mode atomic force microscopy". *Microscopy Research and Technique **65***, 246-251.

Ebner, A., Wildling, L., Kamruzzahan, A. S. M., Rankl, C., Wruss, J., Hahn, C. D., Hölzl, M., Zhu, R., Kienberger, F., Blaas, D., Hinterdorfer, P., and Gruber, H. J. (**2007**) "A new, simple method for linking of antibodies to atomic force microscopy tips". *Bioconjugate Chemistry **18***, 1176-1184.

Eck, M. J., and Sprang, S. R. (**1989**) "The structure of tumor necrosis factor-alpha at 2.6 Å resolution. Implications for receptor binding". *Journal of Biological Chemistry **264***, 17595-17605.

Edinger, R. S., Yospin, J., Perry, C., Kleyman, T. R., and Johnson, J. P. (**2006**) "Regulation of epithelial Na^+ channels (ENaC) by methylation - a novel methyltransferase stimulates ENaC activity". *Journal of Biological Chemistry **281***, 9110-9117.

Eigler, D. M., and Schweizer, E. K. (**1990**) "Positioning single atoms with a scanning tunnelling microscope". *Nature **344***, 524-526.

Elia, N., Tapponnier, M., Matthay, M. A., Hamacher, J., Pache, J.-C., Brundler, M.-A., Totsch, M., De Baetselier, P., Fransen, L., Fukuda, N., Morel, D. R., and Lucas, R. (**2003**) "Functional identification of the alveolar edema reabsorption activity of murine tumor necrosis factor-α". *American Journal of Respiratory and Critical Care Medicine **168***, 1043-1050.

Evans, D. J., Cohen, E. G., and Morriss, G. P. (**1993**) "Probability of second law violations in shearing steady states". *Physical Review Letters **71***, 2401-2404.

Evans, E., and Ritchie, K. (**1997**) "Dynamic strength of molecular adhesion bonds". *Biophysical Journal **72***, 1541-1555.

Farman, N., Talbot, C. R., Boucher, R., Fay, M., Canessa, C., Rossier, B., and Bonvalet, J. P. (**1997**) "Noncoordinated expression of α-, β-, and γ-subunit mRNAs of epithelial Na^+ channel along rat respiratory tract". *American Journal of Physiology Cell Physiology **272***, C131-141.

Fiers, W., Beyaert, R., Boone, E., Cornelis, S., Declercq, W., Decoster, E., Denecker, G., Depuydt, B., De Valck, D., De Wilde, G., Goossens, V., Grooten, J., Haegeman, G., Heyninck, K., Penning, L., Plaisance, S., Vancompernolle, K., Van Criekinge, W., Vandenabeele, P., Vanden Berghe, W., Van de Craen, M., Vandevoorde, V., and Vercammen, D. (**1995**) "TNF-induced intracellular signaling leading to gene induction or to cytotoxicity by necrosis or by apoptosis". *Journal of Inflammation **47***, 67-75.

Fischer, P. M., Krausz, E., and Lane, D. P. (**2001**) "Cellular delivery of impermeable effector molecules in the form of conjugates with peptides capable of mediating membrane translocation". *Bioconjugate Chemistry **12***, 825-841.

Folkesson, H. G., and Matthay, M. A. (**2006**) "Alveolar epithelial ion and fluid transport: recent progress". *American Journal of Respiratory Cell and Molecular Biology **35***, 10-19.

Ford, L. E. (**2010**) "Acute hypertensive pulmonary edema: a new paradigm". *Canadian Journal of Physiology and Pharmacology **88***, 9-13.

Franke, K., Besold, J., Haessler, W., and Seegebarth, C. (**1994**) "Modification and detection of domains on ferroelectric PZT films by scanning force microscopy". *Surface Science **302***, L283-L288.

Fronius, M., and Clauss, W. G. (**2008**) "Mechano-sensitivity of ENaC: may the (shear) force be with you". *Pflugers Archiv - European Journal of Physiology **455***, 775-785.

Garcia-Caballero, A., Ishmael, S. S., Dang, Y., Gillie, D., Bond, J. S., Milgram, S. L., and Stutts, M. J. (**2011**) "Activation of the epithelial sodium channel by the metalloprotease meprin beta subunit". *Channels (Austin) **5***, 14-22.

Garty, H., and Palmer, L. G. (**1997**) "Epithelial sodium channels: function, structure, and regulation". *Physiological Reviews **77***, 359-396.

Gear, C. W. (**1971**) "Numerical initial value problems in ordinary differential equations". **1 ed**., Prentice Hall.

Gibson, C. T., Carnally, S., and Roberts, C. J. (**2007**) "Attachment of carbon nanotubes to atomic force microscope probes". *Ultramicroscopy **107***, 1118-1122.

Giessibl, F. J. (**1995**) "Atomic resolution of the silicon (111)-(7x7) surface by atomic force microscopy". *Science **267***, 68-71.

Gogonea, V., Suarez, D., van der Vaart, A., and Merz, K. W. (**2001**) "New developments in applying quantum mechanics to proteins". *Current Opinion in Structural Biology **11***, 217-223.

Goodsell, D. S., Morris, G. M., and Olson, A. J. (**1996**) "Automated docking of flexible ligands: applications of autodock". *Journal of Molecular Recognition **9***, 1-5.

Grubmüller, H., Heymann, B., and Tavan, P. (**1996**) "Ligand binding: molecular mechanics calculation of the streptavidin-biotin rupture force". *Science **271***, 997-999.

Gschwend, D. A., Good, A. C., and Kuntz, I. D. (**1996**) "Molecular docking towards drug discovery". *Journal of Molecular Recognition **9***, 175-186.

Hamacher, J., Stammberger, U., Roux, J., Kumar, S., Yang, G., Xiong, C., Schmid, R. A., Fakin, R. M., Chakraborty, T., Hossain, H. M. D., Pittet, J.-F., Wendel, A., Black, S. M., and Lucas, R. (**2010**) "The lectin-like domain of tumor necrosis factor improves lung function after rat lung transplantation - potential role for a reduction in reactive oxygen species generation". *Critical Care Medicine **38***, 871-878.

Han, W., Lindsay, S. M., and Jing, T. (**1996**) "A magnetically driven oscillating probe microscope for operation in liquids". *Applied Physics Letters **69***, 4111-4113.

Hazemi, P., Tzotzos, S. J., Fischer, B., Andavan, G. S. B., Fischer, H., Pietschmann, H., Lucas, R., and Lemmens-Gruber, R. (**2010**) "Essential structural features of TNF-α lectin-like domain derived peptides for activation of amiloride-sensitive sodium current in A549 cells". *Journal of Medicinal Chemistry **53***, 8021-8029.

Hehlgans, T., and Pfeffer, K. (**2005**) "The intriguing biology of the tumour necrosis factor/tumour necrosis factor receptor superfamily: players, rules and the games". *Immunology **115***, 1-20.

Herman, S., Loccufier, J., and Schacht, E. (**1994**) "End-group modification of α-hydro-ω-methoxypoly(oxyethylene), 3. Facile methods for the introduction of a thiol-selective reactive end-group". *Macromolecular Chemistry and Physics **195***, 203-209.

Hess, B., Bekker, H., Berendsen, H. J. C., and Fraaije, J. G. E. M. (**1997**) "LINCS: a linear constraint solver for molecular simulations". *Journal of Computational Chemistry **18***, 1463-1472.

Hession, C., Decker, J. M., Sherblom, A. P., Kumar, S., Yue, C. C., Mattaliano, R. J., Tizard, R., Kawashima, E., Schmeissner, U., and Heletky, S. (**1987**) "Uromodulin (Tamm-Horsfall glycoprotein): a renal ligand for lymphokines". *Science **237***, 1479-1484.

Hinterdorfer, P. (**2002**) Molecular recognition studies using the atomic force microscope, In *Atomic Force Microscopy in Cell Biology* (Jena, B. P., and Hörber, J. K. H., Eds.), p 415, Academic Press, San Diego, CA.

Hinterdorfer, P., Baumgartner, W., Gruber, H. J., Schilcher, K., and Schindler, H. (**1996**) "Detection and localization of individual antibody-antigen recognition events by atomic force microscopy". *Proceedings of the National Academy of Sciences of the United States of America **93***, 3477-3481.

Hlodan, R., and Pain, R. H. (**1994**) "Tumour necrosis factor is in equilibrium with a trimeric molten globule at low pH". *FEBS Letters **343***, 256-260.

Ho, K. L., Yusoff, K., Seow, H. F., and Tan, W. S. (**2003**) "Selection of high affinity ligands to hepatitis B core antigen from a phage-displayed cyclic peptide library". *Journal of Medical Virology **69***, 27-32.

Hockney, R. W. (**1970**) "The potential calculation and some applications". *Methods in Computational Physics **9***, 136-211.

Horber, J. K., Haberle, W., Ohnesorge, F., Binnig, G., Liebich, H. G., Czerny, C. P., Mahnel, H., and Mayr, A. (**1992**) "Investigation of living cells in the nanometer regime with the scanning force microscope". *Scanning Microscopy **6***, 919-929.

Hribar, M., Bloc, A., van der Goot, F. G., Fransen, L., De Baetselier, P., Grau, G. E., Bluethmann, H., Matthay, M. A., Dunant, Y., Pugin, J., and Lucas, R. (**1999**) "The lectin-like domain of tumor necrosis factor-alpha increases membrane conductance in microvascular endothelial cells and peritoneal macrophages". *European Journal of Immunology **29***, 3105-3111.

Huberts, D. H. E. W., and van der Klei, I. J. (**2010**) "Moonlighting proteins: An intriguing mode of multitasking". *Biochimica et Biophysica Acta (BBA) - Molecular Cell Research **1803***, 520-525.

Husser, O. E., Craston, D. H., and Bard, A. J. (**1989**) "Scanning electrochemical microscopy". *Journal of the Electrochemical Society **136***, 3222-3229.

Ismailov, I. I., Shlyonsky, V. G., Serpersu, E. H., Fuller, C. M., Cheung, H. C., Muccio, D., Berdiev, B. K., and Benos, D. J. (**1999**) "Peptide inhibition of ENaC". *Biochemistry **38***, 354-363.

Izrailev, S., Stepaniants, S., Balsera, M., Oono, Y., and Schulten, K. (**1997**) "Molecular dynamics study of unbinding of the avidin-biotin complex". *Biophysical Journal **72***, 1568-1581.

Jarzynski, C. (**1997**) "Nonequilibrium equality for free energy differences". *Physical Review Letters **78***, 2690.

Jeffery, C. J. (**1999**) "Moonlighting proteins". *Trends in Biochemical Sciences **24***, 8-11.

Jiang, F., and Kim, S.-H. (**1991**) ""Soft docking": Matching of molecular surface cubes". *Journal of Molecular Biology **219***, 79-102.

Johnson, E. R., and Matthay, M. A. (**2010**) "Acute lung injury: epidemiology, pathogenesis, and treatment". *Journal of Aerosol Medicine and Pulmonary Drug Delivery **23***, 243-252.

Jones, E. Y., Stuart, D. I., and Walker, N. P. (**1989**) "Structure of tumour necrosis factor". *Nature **338***, 225-228.

Kasas, S., and Ikai, A. (**1995**) "A method for anchoring round shaped cells for atomic force microscope imaging". *Biophysical Journal **68***, 1678-1680.

Kashlan, O. B., Boyd, C. R., Argyropoulos, C., Okumura, S., Hughey, R. P., Grabe, M., and Kleyman, T. R. (**2010**) "Allosteric inhibition of the epithelial Na^+ channel through peptide binding at peripheral finger and thumb domains". *Journal of Biological Chemistry **285***, 35216-35223.

Kawagishi, T., Kato, A., Hoshi, Y., and Kawakatsu, H. (**2002**) "Mapping of lateral vibration of the tip in atomic force microscopy at the torsional resonance of the cantilever". *Ultramicroscopy **91***, 37-48.

Kienberger, F., Kada, G., Gruber, H. J., Pastushenko, V. P., Riener, C., Trieb, M., Knaus, H.-G., Schindler, H., and Hinterdorfer, P. (**2000**) "Recognition force spectroscopy studies of the NTA-His6 bond". *Single molecules **1***, 59-65.

Kienberger, F., Pastushenko, V., Kada, G., Puntheeranurak, T., Chtcheglova, A. L., Riethmueller, C., Rankl, C., Ebner, A., and Hinterdorfer, P. (**2006**) "Improving the contrast of topographical AFM images by a simple averaging filter". *Ultramicroscopy **106***, 822-828.

Kleyman, T. R., Carattino, M. D., and Hughey, R. P. (**2009**) "ENaC at the cutting edge: regulation of epithelial sodium channels by proteases". *Journal of Biological Chemistry **284***, 20447-20451.

Krieger, E., Joo, K., Lee, J., Lee, J., Raman, S., Thompson, J., Tyka, M., Baker, D., and Karplus, K. (**2009**) "Improving physical realism, stereochemistry, and side-chain accuracy in homology modeling: four approaches that performed well in CASP8". *Proteins 77*, 114-122.

Krieger, E., Koraimann, G., and Vriend, G. (**2002**) "Increasing the precision of comparative models with YASARA NOVA - a self-parameterizing force field". *Proteins **47***, 393-402.

Krieger, E., Nabuurs, S. B., and Vriend, G. (**2003**) Homology modeling, In *Structural Bioinformatics* (Bourne, P. E., and Weissig, H., Eds.) **1 ed.**, pp 509-525, Wiley-Liss, Hoboken, New Jersey.

Krumrine, J., Raubacher, F., Brooijmans, N., and Kuntz, I. D. (**2003**) Principles and methods of docking and ligand design, In *Structural Bioinformatics* (Bourne, P. E., and Weissig, H., Eds.), pp 443-476, John Wiley and Sons, Hoboken.

Kyte, J., and Doolittle, R. F. (**1982**) "A simple method for displaying the hydropathic character of a protein". *Journal of Molecular Biology **157***, 105-132.

Laskowski, R. A., Macarthur, M. W., Moss, D. S., and Thornton, J. M. (**1993**) "Procheck - a program to check the stereochemical quality of protein structures". *Journal of Applied Crystallography **26***, 283-291.

Le Grimellec, C., Giocondi, M.-C., Pujol, R., and Lesniewska, E. (**2000**) "Tapping mode atomic force microscopy allows the in situ imaging of fragile membrane structures and of intact cells surface at high resolution". *Single molecules **1***, 105-107.

Leach, A. (**2001**) *Molecular modelling: principles and applications*, Prentice Hall.

Lee, G., Chrisey, L., and Colton, R. (**1994**) "Direct measurement of the forces between complementary strands of DNA". *Science **266***, 771-773.

Lu, M., Echeverri, F., Kalabat, D., Laita, B., Dahan, D. S., Smith, R. D., Xu, H., Staszewski, L., Yamamoto, J., Ling, J., Hwang, N., Kimmich, R., Li, P., Patron, E., Keung, W., Patron, A., and Moyer, B. D. (**2008**) "Small molecule activator of the human epithelial sodium channel". *Journal of Biological Chemistry **283***, 11981-11994.

Lucas, R., Magez, S., De Leys, R., Fransen, L., Scheerlinck, J., Rampelberg, M., Sablon, E., and De Baetselier, P. (**1994**) "Mapping the lectin-like activity of tumor necrosis factor". *Science **263***, 814-817.

Lucas, R., Magez, S., Songa, B., Darji, A., Hamers, R., and de Baetselier, P. (**1993**) "A role for TNF during African trypanosomiasis: involvement in parasite control, immunosuppression and pathology". *Immunologic Research **144***, 370-376.

Lucas, R., Verin, A. D., Black, S. M., and Catravas, J. D. (**2009**) "Regulators of endothelial and epithelial barrier integrity and function in acute lung injury". *Biochemical Pharmacology **77***, 1763-1772.

Lundberg, P., and Langel, U. (**2003**) "A brief introduction to cell-penetrating peptides". *Journal of Molecular Recognition **16***, 227-233.

Ma, H. P., Chou, C. F., Wei, S. P., and Eaton, D. C. (**2007**) "Regulation of the epithelial sodium channel by phosphatidylinositides: experiments, implications, and speculations". *Pflügers Archiv - European Journal of Physiology **455***, 169-180.

Maivald, P., Butt, H. J., Gould, S. A. C., Prater, C. B., Drake, B., Gurley, J. A., Elings, V. B., and Hansma, P. K. (**1991**) "Using force modulation to image surface elasticities with the atomic force microscope". *Nanotechnology **2***, 103.

Manassen, Y., Hamers, R. J., Demuth, J. E., and Castellano Jr, A. J. (**1989**) "Direct observation of the precession of individual paramagnetic spins on oxidized silicon surfaces". *Physical Review Letters **62***, 2531.

Marquardt, A., Bernevic, B., and Przybylski, M. (**2007**) "Identification, affinity characterisation and biological interactions of lectin-like peptide-carbohydrate complexes derived from human TNF-α using high-resolution mass spectrometry". *Journal of Peptide Science **13***, 803-810.

Martin, Y., Abraham, D. W., and Wickramasinghe, H. K. (**1988**) "High-resolution capacitance measurement and potentiometry by force microscopy". *Applied Physics Letters **52***, 1103-1105.

Martin, Y., and Wickramasinghe, H. K. (**1987**) "Magnetic imaging by "force microscopy" with 1000 Å resolution". *Applied Physics Letters **50***, 1455-1457.

Martin, Y., Williams, C. C., and Wickramasinghe, H. K. (**1987**) "Atomic force microscope--force mapping and profiling on a sub 100-Å scale". *Journal of Applied Physics **61***, 4723-4729.

Matalon, S., and O'Brodovich, H. (**1999**) "Sodium channels in alveolar epithelial cells: molecular characterization, biophysical properties, and physiological significance". *Annual Review of Physiology **61***, 627-661.

Mate, C. M., McClelland, G. M., Erlandsson, R., and Chiang, S. (**1987**) "Atomic-scale friction of a tungsten tip on a graphite surface". *Physical Review Letters **59***, 1942.

Matthay, M. A., Folkesson, H. G., and Clerici, C. (**2002**) "Lung epithelial fluid transport and the resolution of pulmonary edema". *Physiological Reviews **82***, 569-600.

Matthay, M. A., and Zemans, R. L. (**2011**) "The acute respiratory distress syndrome: pathogenesis and treatment". *Annual Review of Pathology **6***, 147-163.

McCammon, J. A., Gelin, B. R., and Karplus, M. (**1977**) "Dynamics of folded proteins". *Nature **267***, 585-590.

McGuire, M. J., Samli, K. N., Johnston, S. A., and Brown, K. C. (**2004**) "In vitro selection of a peptide with high selectivity for cardiomyocytes in vivo". *Journal of Molecular Biology **342***, 171-182.

Merkel, R., Nassoy, P., Leung, A., Ritchie, K., and Evans, E. (**1999**) "Energy landscapes of receptor-ligand bonds explored with dynamic force spectroscopy". *Nature **397***, 50-53.

Metropolis, N., Rosenbluth, A. W., Rosenbluth, M. N., Teller, A. H., and Teller, E. (**1953**) "Equation of State Calculations by Fast Computing Machines". *Journal of Chemical Physics **21***, 1087-1092.

Miyamoto, S., and Kollman, P. A. (**1992**) "Settle - an analytical version of the shake and rattle algorithm for rigid water models". *Journal of Computational Chemistry **13***, 952-962.

Modelska, K., Matthay, M. A., Brown, L. A., Deutch, E., Lu, L. N., and Pittet, J. F. (**1999**) "Inhibition of beta-adrenergic-dependent alveolar epithelial clearance by oxidant mechanisms after hemorrhagic shock". *American Journal of Physiology **276***, L844-857.

Moitessier, N., Englebienne, P., Lee, D., Lawandi, J., and Corbeil, C. R. (**2008**) "Towards the development of universal, fast and highly accurate docking/scoring methods: a long way to go". *British Journal of Pharmacology **153***, S7-26.

Morris, V. J., Kirby, A. R., and Gunning, A. P. (**2010**) *Atomic force microscopy for biologists*, **2 ed**., Imperial College Press, London.

Mourez, M., Kane, R. S., Mogridge, J., Metallo, S., Deschatelets, P., Sellman, B. R., Whitesides, G. M., and Collier, R. J. (**2001**) "Designing a polyvalent inhibitor of anthrax toxin". *Nature Biotechnology **19***, 958-961.

Murray, J. F. (**2011**) "Pulmonary edema: pathophysiology and diagnosis". *The International Journal of Tuberculosis and Lung Disease **15***, 155-160.

Mutlu, G. M., and Sznajder, J. I. (**2005**) "Mechanisms of pulmonary edema clearance". *American Journal of Physiology Lung Cellular and Molecular Physiology **289***, L685-695.

Nevo, R., Stroh, C., Kienberger, F., Kaftan, D., Brumfeld, V., Elbaum, M., Reich, Z., and Hinterdorfer, P. (**2003**) "A molecular switch between alternative conformational states in the complex of Ran and importin β1". *Nature Structural and Molecular Biology **10***, 553-557.

Nonnenmacher, M., O'Boyle, M. P., and Wickramasinghe, H. K. (**1991**) "Kelvin probe force microscopy". *Applied Physics Letters **58***, 2921-2923.

O'Brodovich, H. (**2005**) "Pulmonary edema in infants and children". *Current Opinion in Pediatrics **17***, 381-384.

O'Keefe, J. A. (**1956**) "Resolving power of visible light". *Journal of the Optical Society of America **46***, 359-359.

Pang, Y.-P., and Kozikowski, A. P. (**1994**) "Prediction of the binding sites of huperzine A in acetylcholinesterase by docking studies". *Journal of Computer-Aided Molecular Design **8***, 669-681.

Pfeiffer, O., Bennewitz, R., Baratoff, A., Meyer, E., and Grutter, P. (**2002**) "Lateral-force measurements in dynamic force microscopy". *Physical Review B **65***, 161403.

Piatigorsky, J. (**2007**) *Gene sharing and evolution*, Harvard University Press.

Piatigorsky, J., O'Brien, W. E., Norman, B. L., Kalumuck, K., Wistow, G. J., Borras, T., Nickerson, J. M., and Wawrousek, E. F. (**1988**) "Gene sharing by delta-crystallin and argininosuccinate lyase". *Proceedings of the National Academy of Sciences of the United States of America **85***, 3479-3483.

Piner, R. D., Zhu, J., Xu, F., Hong, S., and Mirkin, C. A. (**1999**) ""Dip-Pen" nanolithography". *Science **283***, 661-663.

Pohl, D. W., Denk, W., and Lanz, M. (**1984**) "Optical stethoscopy: image recording with resolution λ/20". *Applied Physics Letters **44***, 651-653.

Popp, M. W., Dougan, S. K., Chuang, T. Y., Spooner, E., and Ploegh, H. L. (**2011**) "Sortase-catalyzed transformations that improve the properties of cytokines". *Proceedings of the National Academy of Sciences of the United States of America **108***, 3169-3174.

Preiner, J., Tang, J., Pastushenko, V., and Hinterdorfer, P. (**2007**) "Higher harmonic atomic force microscopy: imaging of biological membranes in liquid". *Physical Review Letters **99***.

Prochiantz, A. (**2011**) "Homeoprotein intercellular transfer, the hidden face of cell-penetrating peptides". *Methods in Molecular Biology **683***, 249-257.

Puntheeranurak, T., Wildling, L., Gruber, H. J., Kinne, R. K. H., and Hinterdorfer, P. (**2006**) "Ligands on the string: single-molecule AFM studies on the interaction of antibodies and substrates with the Na^+-glucose co-transporter SGLT1 in living cells". *Journal of Cell Science **119***, 2960-2967.

Puntheeranurak, T., Wimmer, B., Castaneda, F., Gruber, H. J., Hinterdorfer, P., and Kinne, R. K. H. (**2007**) "Substrate specificity of sugar transport by rabbit SGLT1: single-molecule atomic force microscopy versus transport studies". *Biochemistry **46***, 2797-2804.

Raab, A., Han, W., Badt, D., Smith-Gill, J. S., Lindsay, M. S., Schindler, H., and Hinterdorfer, P. (**1999**) "Antibody recognition imaging by force microscopy". *Nature Biotechnology **17***, 902-905.

Rahman, A., and Stilling.Fh. (**1971**) "Molecular dynamics study of liquid water". *Journal of Chemical Physics **55***, 3336-&.

Renard, S., Voilley, N., Bassilana, F., Lazdunski, M., and Barbry, P. (**1995**) "Localization and regulation by steroids of the alpha, beta and gamma subunits of the amiloride-sensitive Na^+ channel in colon, lung and kidney". *Pflügers Archiv - European Journal of Physiology **430***, 299-307.

Repp, H., Pamukci, Z., Koschinski, A., Domann, E., Darji, A., Birringer, J., Brockmeier, D., Chakraborty, T., and Dreyer, F. (**2002**) "Listeriolysin of *Listeria monocytogenes* forms Ca^{2+}-permeable pores leading to intracellular Ca^{2+} oscillations". *Cellular Microbiology **4***, 483-491.

Riener, C. K., Stroh, C. M., Ebner, A., Klampfl, C., Gall, A. A., Romanin, C., Lyubchenko, Y. L., Hinterdorfer, P., and Gruber, H. J. (**2003**) "Simple test system for single molecule recognition force microscopy". *Analytica Chimica Acta **479***, 59-75.

Rimoldi, S. F., Yuzefpolskaya, M., Allemann, Y., and Messerli, F. (**2009**) "Flash pulmonary edema". *Progress in Cardiovascular Diseases **52***, 249-259.

Ryckaert, J.-P., Ciccotti, G., and Berendsen, H. J. C. (**1977**) "Numerical integration of the cartesian equations of motion of a system with constraints: molecular dynamics of n-alkanes". *Journal of Computational Physics **23***, 327-341.

Saenz, J. J., Garcia, N., Grutter, P., Meyer, E., Heinzelmann, H., Wiesendanger, R., Rosenthaler, L., Hidber, H. R., and Guntherodt, H.-J. (**1987**) "Observation of magnetic forces by the atomic force microscope". *Journal of Applied Physics **62***, 4293-4295.

Sakuma, T., Folkesson, H. G., Suzuki, S., Okaniwa, G., Fujimura, S., and Matthay, M. A. (**1997**) "Beta-adrenergic agonist stimulated alveolar fluid clearance in ex vivo human

and rat lungs". *American Journal of Respiratory and Critical Care Medicine **155***, 506-512.

Sandak, B., Nussinov, R., and Wolfson, H. J. (**1995**) "An automated computer vision and robotics-based technique for 3-D flexible biomolecular docking and matching". *Computer Applications in the Biosciences **11***, 87-99.

Scott, C. P., Abel-Santos, E., Wall, M., Wahnon, D. C., and Benkovic, S. J. (**1999**) "Production of cyclic peptides and proteins in vivo". *Proceedings of the National Academy of Sciences of the United States of America **96***, 13638-13643.

Sherblom, A. P., Decker, J. M., and Muchmore, A. V. (**1988**) "The lectin-like interaction between recombinant tumor necrosis factor and uromodulin". *Journal of Biological Chemistry **263***, 5418-5424.

Schlick, T. (**2010**) *Molecular modeling and simulation: an interdisciplinary guide*, **2 ed.**, Springer, New York.

Schmalz, G. (**1929**) "Uber Glätte und Ebenheit als physikalisches und physiologishes Problem". *Zeitschrift des Vereines deutscher Ingenieure*, 1461-1467.

Sticht, J., Humbert, M., Findlow, S., Bodem, J., Muller, M., Dietrich, U., Werner, J., and Krausslich, H. G. (**2005**) "A peptide inhibitor of HIV-1 assembly in vitro". *Nature Structural and Molecular Biology **12***, 671-677.

Strunz, T., Oroszlan, K., Schäfer, R., and Güntherodt, H.-J. (**1999**) "Dynamic force spectroscopy of single DNA molecules". *Proceedings of the National Academy of Sciences of the United States of America **96***, 11277-11282.

Svenningsen, P., Friis, U. G., Bistrup, C., Buhl, K. B., Jensen, B. L., and Skott, O. (**2011**) "Physiological regulation of epithelial sodium channel by proteolysis". *Current Opinion in Nephrology and Hypertension **20***, 529-533.

Swope, W. C., Andersen, H. C., Berens, P. H., and Wilson, K. R. (**1982**) "A computer-simulation method for the calculation of equilibrium-constants for the formation of physical clusters of molecules – application to small water clusters". *Journal of Chemical Physics **76***, 637-649.

Synge, E. H. (**1928**) "A suggested method for extending microscopic resolution into the ultra-microscopic region". *Philosophical Magazine **6***, 356 - 362.

Synge, E. H. (**1932**) "An application of piezo-electricity to microscopy". *Philosophical Magazine **13***, 297 - 300.

Takata, K., Kushida, K., Torii, K., and Miki, H. (**1994**) "Strain imaging of lead-zirconate-titanate thin film by tunneling acoustic microscopy". *Japanese Journal of Applied Physics **33***, 3193.

Trott, O., and Olson, A. J. (**2009**) "AutoDock Vina: Improving the speed and accuracy of docking with a new scoring function, efficient optimization, and multithreading". *Journal of Computational Chemistry **31***, 455-461.

Turner, R. D., Kirkham, J., Devine, D., and Thomson, N. H. (**2009**) "Second harmonic atomic force microscopy of living *Staphylococcus aureus* bacteria". *Applied Physics Letters **94***.

Ussing, H. H., and Zerahn, K. (**1951**) "Active transport of sodium as the source of electric current in the short-circuited isolated frog skin". *Acta Physiologica Scandinavica **23***, 110-127.

Vadász, I., Schermuly, R. T., Ghofrani, H. A., Rummel, S., Wehner, S., Mühldorfer, I., Schäfer, K. P., Seeger, W., Morty, R. E., Grimminger, F., and Weissmann, N. (**2008**) "The lectin-like domain of tumor necrosis factor-α improves alveolar fluid balance in injured isolated rabbit lungs". *Critical Care Medicine **36***, 1543-1550.

Vakser, I. A. (**1995**) "Protein docking for low-resolution structures". *Protein Engineering Design and Selection **8***, 371-377.

van der Goot, F. G., Pugin, J., Hribar, M., Fransen, L., Dunant, Y., De Baetselier, P., Bloc, A., and Lucas, R. (**1999**) "Membrane interaction of TNF is not sufficient to trigger increase in membrane conductance in mammalian cells". *FEBS Letters **460***, 107-111.

van Nieuw Amerongen, G. P., Vermeer, M. A., and van Hinsbergh, V. W. (**2000**) "Role of RhoA and Rho kinase in lysophosphatidic acid-induced endothelial barrier dysfunction". *Arteriosclerosis, Thrombosis, and Vascular Biology **20***, E127-133.

Vassalli, P. (**1992**) "The pathophysiology of tumor necrosis factors". *Annual Review of Immunology **10***, 411-452.

Verlet, L. (**1967**) "Computer experiments on classical fluids .I. Thermodynamical properties of Lennard-Jones molecules". *Physical Review **159***, 98-&.

Voilley, N., Lingueglia, E., Champigny, G., Mattei, M. G., Waldmann, R., Lazdunski, M., and Barbry, P. (**1994**) "The lung amiloride-sensitive Na^+ channel: biophysical properties, pharmacology, ontogenesis, and molecular cloning". *Proceedings of the National Academy of Sciences of the United States of America **91***, 247-251.

Wallach, D., Varfolomeev, E. E., Malinin, N. L., Goltsev, Y. V., Kovalenko, A. V., and Boldin, M. P. (**1999**) "Tumor necrosis factor receptor and Fas signaling mechanisms". *Annual Review of Immunology **17***, 331-367.

Walls, P. H., and Sternberg, M. J. E. (**1992**) "New algorithm to model protein protein recognition based on surface complementarity – applications to antibody antigen docking". *Journal of Molecular Biology **228***, 277-297.

Wang, G. M., Sevick, E. M., Mittag, E., Searles, D. J., and Evans, D. J. (**2002**) "Experimental demonstration of violations of the second law of thermodynamics for small systems and short time scales". *Physical Review Letters **89***, 050601.

Ware, L. B., and Matthay, M. A. (**2005**) "Clinical practice. Acute pulmonary edema". *The New England Journal of Medicine **353***, 2788-2796.

Wiesehan, K., Buder, K., Linke, R. P., Patt, S., Stoldt, M., Unger, E., Schmitt, B., Bucci, E., and Willbold, D. (**2003**) "Selection of D-Amino-Acid peptides that bind to Alzheimer's disease amyloid peptide A beta(1-42) by mirror image phage display". *ChemBioChem **4***, 748-753.

Wildling, L., Rankl, C., Haselgruebler, T., Gruber, H. J., Holy, M., Newman, A. H., Zou, M. F., Zhu, R., Freissmuth, M., Sitte, H. H., and Hinterdorfer, P. (**2011**) "Probing the binding pocket of the serotonin transporter by single molecular force spectroscopy on living cells". *Journal of Biological Chemistry*.

Williams, C. C., and Wickramasinghe, H. K. (**1986**) "Scanning thermal profiler". *Applied Physics Letters **49***, 1587-1589.

Xiong, C., Yang, G., Kumar, S., Aggarwal, S., Leustik, M., Snead, C., Hamacher, J., Fischer, B., Umapathy, N. S., Hossain, H., Wendel, A., Catravas, J. D., Verin, A. D., Fulton, D., Black, S. M., Chakraborty, T., and Lucas, R. (**2010**) "The lectin-like domain of TNF protects from listeriolysin-induced hyperpermeability in human pulmonary microvascular endothelial cells – a crucial role for protein kinase C-α inhibition". *Vascular Pharmacology **52***, 207-213.

Xu, S., and Liu, G.-y. (**1997**) "Nanometer-scale fabrication by simultaneous nanoshaving and molecular self-assembly". *Langmuir **13***, 127-129.

Young, R., Ward, J., and Scire, F. (**1972**) "The topografiner: an instrument for measuring surface microtopography". *Review of Scientific Instruments **43***, 999-1011.

Yuriev, E., Agostino, M., and Ramsland, P. A. (**2010**) "Challenges and advances in computational docking: 2009 in review". *Journal of Molecular Recognition **24***, 149-164.

Zhang, Y. K. (**2006**) "Pseudobond ab initio QM/MM approach and its applications to enzyme reactions". *Theoretical Chemistry Accounts **116***, 43-50.